
A HIGHER ORDER LOCAL MESH METHOD FOR APPROXIMATING LAPLACIANS ON UNKNOWN MANIFOLDS

A PREPRINT

John Wilson Peoples

Department of Mathematics
The Pennsylvania State University, University Park, PA 16802, USA
jwp5828@psu.edu

John Harlim

Department of Mathematics, Department of Meteorology and Atmospheric Science,
Institute for Computational and Data Sciences
The Pennsylvania State University, University Park, PA 16802, USA
jharlim@psu.edu

May 27, 2024

ABSTRACT

In this work, we introduce a numerical method for approximating arbitrary differential operators on vector fields in the weak form given point cloud data sampled randomly from a d dimensional manifold embedded in \mathbb{R}^n . This method generalizes the local linear mesh method to the local curved mesh method, thus, allowing for the estimation of differential operators with nontrivial Christoffel symbols, such as the Bochner or Hodge Laplacians. In particular, we leverage the potentially small intrinsic dimension of the manifold ($d \ll n$) to construct local parameterizations that incorporate both local meshes and higher-order curvature information. The former is constructed using low dimensional meshes obtained from local data projected to the tangent spaces, while the latter is obtained by fitting local polynomials with the generalized moving least squares. Theoretically, we prove the weak and spectral convergence rates for the proposed method for the estimation of the Bochner Laplacian. We provide numerical results supporting the theoretical convergence rates for the Bochner and Hodge Laplacians on simple manifolds.

1 Introduction

The numerical approximation of differential operators based on a point cloud (i.e., a set of points lying on a manifold embedded in Euclidean space) is a fundamental problem in mathematics with numerous applications ranging from image processing [31, 27, 5, 22], computer graphics [6, 35, 23], granular flow [26], phase formation [12], liquid crystals [25] and biomembranes [15]. However, when the point cloud is randomly sampled from a low dimensional manifold embedded in high dimensional Euclidean space, traditional approaches, such as finite element methods, suffer from the curse of ambient dimension, as well as the random distribution of nodes and expensive construction of potentially global meshes in the high dimensional ambient space.

A fundamental class of algorithms aims to solve the above problem by constructing a graph Laplacian matrix, leveraging the heat kernel, to estimate the Laplacian operator from the pairwise affinity of points. While such methods leverage the intrinsic dimension of the manifold to avoid the ambient dimension, they lack flexibility in estimating operators other than the Laplacian. Specifically, the Laplacian eigenmaps [1], diffusion maps algorithm [10], consistently approximates the Laplace-Beltrami operator (see e.g., [2, 28, 4, 8]). The vector diffusion maps [29] generalizes the diffusion maps to include local parallel transport in the kernel and shows consistency in approximating the Connection Laplacian. Beyond these purely graph-Laplacian approximations, a Galerkin-based method called the Spectral Exterior Calculus (SEC) has been proposed to approximate Hodge Laplacian on 1-forms

[3]. The accuracy of the SEC depends on the method used in the estimation of the zero Laplacian since this approach represents differential forms (and vector fields) with a Galerkin expansion of eigensolutions of the Laplace-Beltrami operator.

A general mesh-free technique for estimating differential operators on tensor fields has been proposed in [16] where the presented RBF interpolant in that paper can be replaced with a computationally more efficient interpolant (with sparse interpolation matrix), such as the generalized least squares (GMLS), as shown in [21, 17]. This method leverages moving least squares to estimate local charts and, subsequently, approximates differential operators using standard pointwise local formulas in differential geometry. Since these approaches are based on the pointwise formulation, they produce a non-symmetric estimation of Laplacians, which significantly complicates both the computations and theoretical analysis. Moreover, due to its mesh-less nature, the variational formulation is always biased by the Monte-Carlo approximation [16]. To overcome this issue, the work in [18] proposes fitting differential operators in variational formulation to linear local meshes constructed from the projections of points to the estimated tangent spaces induced by the point cloud data. This framework allows one to construct symmetric estimations for a flexible array of differential operators, as well as estimations of other intrinsic quantities. However, the estimated metric in this framework is constant on each triangle in the local meshes. Therefore, this method fails to approximate operators whose local formulas depend on higher-order curvature quantities, such as Christoffel symbols. One example of such an operator is the Bochner Laplacian.

In this paper, we leverage the higher order estimations of [21], along with the local mesh framework of [18] to obtain symmetric estimations of arbitrary differential operators on tensor fields with theoretical convergence guarantees. Namely, we generalize the local variational formulation Laplace-Beltrami to arbitrary vector Laplacians where the local linear mesh proposed in [18] is generalized to curved local mesh estimated using the generalized least squares parameterization as in [21]. Using this framework, we prove weak and spectral consistency to the Bochner Laplacian in the limit of large data. Furthermore, detailed numerical investigations verify the convergence of Hodge and Bochner Laplacian estimations obtained from randomly sampled ambient point cloud data.

The remainder of this paper is organized as follows. In Section 2, we review the local frameworks of [18] and [21]. We also demonstrate how the parameterization of [21] can be used on the local mesh of [18] to obtain local curved meshes. In Section 3, we formulate how the local charts of Section 2 can be used to obtain weak form estimations of arbitrary differential operators on tensor fields. In Section 4, we prove theoretical convergence guarantees for the estimation of energy, as well as eigenvalues. Finally, in Section 5, we demonstrate the numerical convergence of the local curved mesh method in estimating the Hodge and Bochner Laplacians on some example manifolds.

2 Local Metric Learning

This section provides an overview of two existing frameworks which are key to the novel method introduced in this paper. We begin by giving a description of the Local Mesh Method [18], which leverages local tangent space approximations to construct triangular meshes near each element of a given point cloud. We also present a brief overview of the Generalized Moving Least Squares technique [21], in which local parameterizations of the form $\Phi : T_x M \rightarrow M$ are approximated by fitting polynomials on the estimated tangent spaces using a weighted least squares. Subsequently, we introduce the Local Curved Mesh Method, which serves as the central idea of this paper, amalgamating the aforementioned methodologies. To allow for a concise description of each method, we focus on learning the Riemannian metric of an unknown manifold on a local chart throughout this section. The ideas of this section, however, can be extended to approximate more complicated objects on manifold (e.g., operators on tensor bundles, as shown in Section 3). We supplement this paper with two appendices: In Appendix A, we report the detailed calculation for the components of the mass and stiffness matrices for both the Bochner and Hodge Laplacians. In Appendix B, we report the proofs of some technical lemmas.

2.1 Local tangent space approximation

Given a point cloud $X = \{x_1, \dots, x_N\} \subseteq \mathbb{R}^n$ sampled from an unknown manifold M of dimension $d \ll n$, we wish to obtain local estimation of $T_{x_i} M$, the tangent space at each point, as each method of locally approximating a Riemannian metric described in this section hinges on such an estimation. This problem is well studied in the literature, and is frequently addressed using local SVD [13, 32, 34] or local PCA, as in [18, 21]. More recently, a 2nd order local SVD method introduced in [16] improves on local SVD by keeping track of higher order terms. For simplicity, we provide a brief overview of local PCA.

Given a point x_i , denote its k nearest neighbors by $K(i) = \{x_{i_1}, \dots, x_{i_k}\}$. In this notation, $x_i = x_{i_1}$. Consider the local $n \times n$ covariance matrix

$$P_i = \sum_{x \in K(i)} (x - \mu_i)(x - \mu_i)^\top,$$

where $\mu_i = \frac{1}{k} \sum_{x \in K(i)} x$. In practice, we found insignificant accuracy differences using either the average μ_i or the base point x_i in placing μ_i away from the boundary. After diagonalizing this matrix, one obtains n eigenpairs $(\lambda_1^{(i)}, \mathbf{t}_1^{(i)}), \dots, (\lambda_n^{(i)}, \mathbf{t}_n^{(i)})$ with $\lambda_j^{(i)} \geq \lambda_{j+1}^{(i)}$. Since the intrinsic dimension of the data is d , one expects to find that

$$\lambda_1^{(i)} \geq \lambda_2^{(i)} \geq \dots \geq \lambda_d^{(i)} \gg \lambda_{d+1}^{(i)},$$

given that the sampling is sufficiently dense around x_i . Thus, one can determine the dimension d , and obtains an orthonormal basis $\{\mathbf{t}_1^{(i)}, \dots, \mathbf{t}_d^{(i)}\}$ estimating the tangent space at x_i . We denote the copy of \mathbb{R}^d given by the span of these coordinates by $\overline{T_{x_i} M}$. In what follows, we assume such an estimation is obtained, and denote the basis vectors as above.

2.2 Approximation of metric tensor with linear local meshes

Given x_i , we aim to obtain a d -dimensional mesh for $K(i)$, which is x_i and its k -nearest neighbors. To simplify the discussion, we assume $d = 2$. In [18], they propose to solve this problem by first projecting $K(i)$ to the estimated tangent space:

$$T(i) := \left\{ \underbrace{\left(\mathbf{t}_1^{(i)} \cdot (x_{i_1} - x_{i_1}), \mathbf{t}_2^{(i)} \cdot (x_{i_1} - x_{i_1}) \right)}_{(0,0)=\vec{0}}, \dots, \left(\mathbf{t}_1^{(i)} \cdot (x_{i_k} - x_{i_1}), \mathbf{t}_2^{(i)} \cdot (x_{i_k} - x_{i_1}) \right) \right\} \subseteq \overline{T_{x_i} M}.$$

For simplicity of future notation, we define

$$\vec{v}_{i_r} = \begin{pmatrix} \mathbf{t}_1^{(i)} \cdot (x_{i_r} - x_{i_1}) \\ \mathbf{t}_2^{(i)} \cdot (x_{i_r} - x_{i_1}) \end{pmatrix}, \quad (1)$$

so that

$$T(i) = \{\vec{v}_{i_1} = \vec{0}, \vec{v}_{i_2}, \dots, \vec{v}_{i_k}\}.$$

A mesh on $T(i)$, denoted by $\mathbf{R}(i)$, is obtained using standard methods, e.g., the Delaunay triangulation. Denote by $R(i)$ the first ring of this triangulation, that is, $R(i)$ is set of ℓ triangles of this mesh which include the basepoint $(0, 0)$. These necessarily take the form

$$R(i) = \{T_{i,1}, \dots, T_{i,\ell}\} \subset \mathbf{R}(i),$$

where each $T_{i,r} = [\vec{0}, \vec{v}_{i_{j_r}}, \vec{v}_{i_{k_r}}]$. Consider any such triangle. This can be parameterized by the standard Barycentric parameterization with the canonical right triangle $T = \{(u_1, u_2) | u_1, u_2 \geq 0, u_1 + u_2 \leq 1\}$ via the map $\Phi_{T_{i,r}} : T \rightarrow T_{i,r} \subseteq \mathbb{R}^d$ defined by

$$(u_1, u_2) \mapsto u_1 \vec{v}_{i_{j_r}} + u_2 \vec{v}_{i_{k_r}}. \quad (2)$$

Since the first ring can be "lifted" from the tangent space to the manifold via the one-to-one correspondence between $T(i)$ and $K(i)$ given by

$$\vec{v}_{i_r} \mapsto x_{i_r}.$$

we obtain the map to the global coordinates, $\tilde{\Phi}_{T_{i,r}} : T \rightarrow \mathbb{R}^n$, defined by

$$(u_1, u_2) \mapsto u_1(x_{i_{j_r}} - x_i) + u_2(x_{i_{k_r}} - x_i) + x_i. \quad (3)$$

Let $y \in \tilde{\Phi}_{T_{i,r}}(T) \subset \mathbb{R}^n$. Based on the barycentric parameterization, there exists $(u_1, u_2) \in T$ such that

$$y = (1 - u_1 - u_2)x_i + u_1 x_{i_{j_r}} + u_2 x_{i_{k_r}} = x_i + u_1(x_{i_{j_r}} - x_i) + u_2(x_{i_{k_r}} - x_i) := \tilde{\Phi}_{T_{i,r}}(u_1, u_2),$$

which is effectively Eq (3) above. From this identity, it is clear that,

$$\underbrace{[\mathbf{t}_1^{(i)} \mathbf{t}_2^{(i)}]^\top}_{=\mathbf{T}^\top} (y - x_i) = u_1 \vec{v}_{i_{j_r}} + u_2 \vec{v}_{i_{k_r}} = \tilde{\Phi}_{T_{i,r}}(u_1, u_2).$$

Then

$$y - x_i = \mathbf{T}\mathbf{T}^\top (y - x_i) + \mathbf{t}_3^{(i)} \mathbf{t}_3^{(i)\top} (y - x_i),$$

so we can obtain the relation between $\tilde{\Phi}$ in terms of Φ ,

$$\tilde{\Phi}_{T_{i,r}}(u_1, u_2) = \mathbf{T}\Phi_{T_{i,r}}(u_1, u_2) + \mathbf{t}_3^{(i)} \mathbf{t}_3^{(i)\top} (y - x_i) + x_i. \quad (4)$$

In this case, the 'lifted' triangle can be understood as a linear interpolation in the normal component given by,

$$p_{i,r}(u_1, u_2) = \mathbf{t}_3^{(i)\top} (y - x_i) = u_1 \mathbf{t}_3^{(i)\top} (x_i - x_{i_{j_r}}) + u_2 \mathbf{t}_3^{(i)\top} (x_i - x_{i_{k_r}}),$$

where $p_{i,r} : T \rightarrow \mathbb{R}^{n-d}$ is a linear function.

The coordinates corresponding to the map $\tilde{\Phi}_{T_{i,r}}$ is then given by,

$$\left\{ \partial_{u_1} = x_{i_{j_r}} - x_i, \partial_{u_2} = x_{i_{k_r}} - x_i \right\}$$

in which the Riemannian metric takes the form

$$\mathbf{g}_{\tilde{\Phi}_{T_{i,r}}}(u_1, u_2) = \begin{bmatrix} \|x_{i_{j_r}} - x_i\|^2 & (x_{i_{j_r}} - x_i) \cdot (x_{i_{k_r}} - x_i) \\ (x_{i_{k_r}} - x_i) \cdot (x_{i_{j_r}} - x_i) & \|x_{i_{k_r}} - x_i\|^2 \end{bmatrix}. \quad (5)$$

We emphasize that in this formulation, the Riemannian metric is constant as a matrix valued function of (u_1, u_2) . The work in [18] leverages these coordinate representations, along with local coordinate invariant formulas, to approximate other geometric objects, such as the Laplace-Beltrami operator.

Remark 1. *Since the above metric formula is constant in (u_1, u_2) , it is clear that operator defines on the above local mesh parameterization cannot distinguish operators that are differed by higher order objects (e.g., the Hodge and Bochner Laplacians are differed by Ricci curvature). This issue, which arises from the trivial Cristoffel symbols in this linear mesh parameterization, motivates the use of curving (non-flat) local meshes as discussed in Section 2.4. In Section 3, we will demonstrate how such a general (curving) local mesh framework can be used to learn operators on general tensor fields.*

2.3 Generalized moving least squares approximation

Without loss of generality, we set $d = 2$ and $n = 3$ to simplify the discussion. Details for extending these ideas to the more general setting can be found in [21]. Given a point x_i , consider the basis $\{\mathbf{t}_1^{(i)}, \mathbf{t}_2^{(i)}, \mathbf{t}_3^{(i)}\}$, where $\{\mathbf{t}_1^{(i)}, \mathbf{t}_2^{(i)}\}$ is a basis for the approximated tangent space $T_{x_i}M$, and $\mathbf{t}_3^{(i)}$ approximates the normal direction. Recall that the k nearest neighbors $K(i)$, and the neighbors projected onto the tangent space $T(i)$. Denote by $N(i)$ the normal components:

$$N(i) := \left\{ \mathbf{t}_3^{(i)} \cdot (x_{i_1} - x_i), \dots, \mathbf{t}_3^{(i)} \cdot (x_{i_k} - x_i) \right\}.$$

Consider a polynomial $p_i : \overline{T_{x_i}M} \rightarrow \mathbb{R}^{n-d}$ defined by

$$p_i(v_1, v_2) = av_1^2 + bv_2^2 + cv_1v_2 + dv_1 + ev_2 + f, \quad (6)$$

where the coefficients are obtained by a weighted least squares fit to the data in $T(i)$ with labels given by $N(i)$. In particular, the coefficients are obtained via

$$(a, b, c, d, e, f) = \operatorname{argmin} \sum_{j=1}^k \omega(\|x_i - x_{i_j}\|) \left(p_i(\bar{v}_{i_j}) - \mathbf{t}_3^{(i)} \cdot (x_{i_j} - x_i) \right)^2 \quad (7)$$

for some weight function ω , where \bar{v}_{i_j} is as defined in Equation (1). Following [20, 21], we will consider only the weight function

$$\omega(t) = \begin{cases} 1 & t = 0 \\ 1/k & \text{else,} \end{cases}$$

which is empirically found to be adequate for random data. After fitting such a polynomial, we obtain a local parameterization of the form

$$\alpha_{x_i} : (v_1, v_2) \mapsto (v_1, v_2, p_i(v_1, v_2)). \quad (8)$$

This parameterization induces the following coordinates:

$$\left\{ \partial_{v_1} = \begin{bmatrix} 1 \\ 0 \\ 2av_1 + cv_2 + d \end{bmatrix}, \partial_{v_2} = \begin{bmatrix} 0 \\ 1 \\ 2bv_2 + cv_1 + e \end{bmatrix} \right\}.$$

such that the Riemannian metric in these coordinates takes the form,

$$g_{x_i}(v_1, v_2) = \begin{bmatrix} 1 + (2av_1 + cv_2 + d)^2 & (2av_1 + cv_2 + d)(2bv_2 + cv_1 + e) \\ (2av_1 + cv_2 + d)(2bv_2 + cv_1 + e) & 1 + (2bv_2 + cv_1 + e)^2 \end{bmatrix}.$$

We remark that while the domain of the parameterization from the previous subsection is a standard simplex, the domain of the parameterization from this subsection is the estimated tangent space itself.

2.4 Approximation of metric tensor with local curved meshes

Local curved meshes conceptually combine the quadratic parameterization of the previous section with the local meshes of Section 2.2. As we shall see in Section 3, this approximation allows the flexibility and robustness in using random data in the weak approximation of differential operators while simultaneously avoiding the issues mentioned in Remark 1. To this end, consider a fixed point x_i , and its first ring $R(i)$. For an arbitrary triangle

$$T_{i,r} = [0, \vec{v}_{i_{j_r}}, \vec{v}_{i_{k_r}}] \in R(i),$$

recall the map $\Phi_{T_{i,r}}$ as defined in Equation 2. The codomain of this map is $\overline{T_{x_i}M}$, which is precisely the domain of the parameterization p_i from the previous section. Hence, it's natural to consider parameterizations $\tilde{\Phi}_{C_{i,r}} : T \rightarrow \mathbb{R}^n$ of the curved triangular patches of the locally approximated manifold, given by,

$$\tilde{\Phi}_{C_{i,r}}(u_1, u_2) = \mathbf{T}\Phi_{T_{i,r}}(u_1, u_2) + \mathbf{t}_3^{(i)} p_{i,r}(u_1, u_2) + x_i, \quad (9)$$

where we generalize (4) by setting the vertical component $p_{i,r} : T \rightarrow \mathbb{R}^n$ to be a nonlinear map,

$$p_{i,r}(u_1, u_2) = p_i \circ \Phi_{T_{i,r}}(u_1, u_2),$$

where p_i is obtained by the generalized moving least-squares procedure discussed in Section 2.3. The map $\tilde{\Phi}_{C_{i,r}}$ is effectively a generalization of $\Phi_{T_{i,r}}$, where we embed a curved (non-flat) mesh in \mathbb{R}^n using a nonlinear map $p_{i,r}$.

Based on this map, one can construct the Riemannian metric $g_{\tilde{\Phi}_{C_{i,r}}}$ corresponding to the curved mesh, generalizing (5). Since the computation will be done locally for each based point x_i , it is more convenient to implement the construction without mapping to the global coordinates with the following,

$$\Phi_{C_{i,r}}(u_1, u_2) := \begin{pmatrix} \Phi_{T_{i,r}}(u_1, u_2) \\ p_i \circ \Phi_{T_{i,r}}(u_1, u_2) \end{pmatrix}. \quad (10)$$

This results in coordinates

$$\left\{ \partial_{u_1} = \begin{bmatrix} \vec{v}_{i_{j_r}} \\ \nabla p_i(\Phi_{T_{i,r}}(u_1, u_2)) \cdot \vec{v}_{i_{j_r}} \end{bmatrix}, \partial_{u_2} = \begin{bmatrix} \vec{v}_{i_{k_r}} \\ \nabla p_i(\Phi_{T_{i,r}}(u_1, u_2)) \cdot \vec{v}_{i_{k_r}} \end{bmatrix} \right\} \quad (11)$$

In these coordinates, the Riemannian metric takes the form

$$g_{\Phi_{C_{i,r}}}(u_1, u_2) = \begin{bmatrix} \|\vec{v}_{i_{j_r}}\|^2 & \vec{v}_{i_{j_r}} \cdot \vec{v}_{i_{k_r}} \\ \vec{v}_{i_{j_r}} \cdot \vec{v}_{i_{k_r}} & \|\vec{v}_{i_{k_r}}\|^2 \end{bmatrix} + \begin{bmatrix} \left(\nabla p_i(\Phi_{T_{i,r}}(u_1, u_2)) \cdot \vec{v}_{i_{j_r}} \right)^2 & c_{j_r k_r}^i(u_1, u_2) \\ c_{j_r k_r}^i(u_1, u_2) & \left(\nabla p_i(\Phi_{T_{i,r}}(u_1, u_2)) \cdot \vec{v}_{i_{k_r}} \right)^2 \end{bmatrix} \quad (12)$$

where $c_{j_r k_r}^i(u_1, u_2) = \left(\nabla p_i(\Phi_{T_{i,r}}(u_1, u_2)) \cdot \vec{v}_{i_{j_r}} \right) \cdot \left(\nabla p_i(\Phi_{T_{i,r}}(u_1, u_2)) \cdot \vec{v}_{i_{k_r}} \right)$.

3 Operator Approximation in Weak Form

The local mesh method of [18], and hence the curved mesh method described in Section 2.4 lends itself to weak operator approximations, analogous to finite element frameworks. While the work in [18] outlines such approach in approximating the Laplace-Beltrami operator (on functions), the same framework can be generalized to differential operators on tensor fields. For instance, this framework can be used to estimate the Laplacian on vector fields. In this section, we outline this process. We begin by describing how the Laplace-Beltrami operator can be estimated, pointing out the key differences between [18] and the curved mesh method. We then generalize this, in the case of the curved mesh method, to arbitrary operators on tensor fields. Since operators on vector fields, such as the Bochner and Hodge Laplacians, are of particular interest, we supply additional details for these cases.

3.1 Weak approximation of the Laplace-Beltrami operator

Consider a nodal basis of functions $\{e_i : M \rightarrow \mathbb{R}\}_{i=1}^N$ satisfying the property

$$e_i(x_j) = \delta_{ij},$$

so that an arbitrary function $f : X \rightarrow \mathbb{R}$ can be interpolated as

$$f(x) = \sum_{i=1}^N f(x_i) e_i(x).$$

For each pair (x_i, x_j) consider the quantity

$$S_{ij} := \int_M \langle \nabla e_i, \nabla e_j \rangle_g d\text{Vol} \approx \sum_{T_{i,r} \in R(i)} \int_T \langle \nabla_{\Psi_{i,r}} e_i, \nabla_{\Psi_{i,r}} e_j \rangle_{g_{\Psi_{i,r}}} \sqrt{\det(g_{\Psi_{i,r}})} du_1 du_2, \quad (13)$$

where $\nabla_{\Psi_{i,r}}$ and $g_{\Psi_{i,r}}$ denote the gradient and Riemannian metric, respectively, with each computed in the coordinates of some parameterization $\Psi_{i,r} : T \rightarrow \mathbb{R}^n$. In (13), the integration is locally approximated on local meshes induced by the parameterization $\Psi_{i,r}$. For instance, for the original (flat) local mesh method, the corresponding parameterization is given by Equation (3), whereas for the curved mesh method the parameterization is given by Equation (10).

When the nodal basis is given by hat functions (i.e., when $e_i(u_1, u_2) = 1 - u_1 - u_2$ in the coordinates of $\Psi_{T_{i,r}} : T \rightarrow \mathbb{R}^n$) and the parameterization is given by (3), $\Psi_{T_{i,r}} = \tilde{\Phi}_{T_{i,r}}$, the only nonzero terms in the above sum are when $i = j$ or when $\bar{x}_i \bar{x}_j$ is a side in the lifted triangulation of $T(i)$. Such integrals can be computed analytically. In fact, when hat functions are used, this is formula results in the famous cotangent formula for the Laplace-Beltrami operator [14]. Denote by \mathbf{S} the $N \times N$ sparse matrix with (i, j) -th entry $(\mathbf{S})_{ij} = S_{ij}$. Similarly, denote by \mathbf{M} the sparse matrix with entries

$$M_{ij} := \sum_{T_{i,r} \in R(i)} \int_T e_i(u_1, u_2) e_j(u_1, u_2) \sqrt{\det(g_{\Psi_{i,r}})} du_1 du_2. \quad (14)$$

By definition, it is not necessarily true that $S_{ij} = S_{ji}$. Following [18], we define symmetric matrices, $\mathbf{A} = \frac{1}{2}(\mathbf{S} + \mathbf{S}^\top)$, and $\mathbf{B} = \frac{1}{2}(\mathbf{M} + \mathbf{M}^\top)$, and approximate the weak form Laplace-Beltrami eigenvalue problem,

$$\int_M \langle \nabla f, \nabla f \rangle_g d\text{Vol} = \lambda \int_M f^2 d\text{Vol}$$

with

$$\langle \mathbf{A}\mathbf{f}, \mathbf{f} \rangle = \lambda \langle \mathbf{B}\mathbf{f}, \mathbf{f} \rangle,$$

where $\mathbf{f} = (f(x_1), \dots, f(x_N))^\top$ and $\langle \cdot, \cdot \rangle$ denotes the Euclidean dot product (which will be used accordingly for the remainder of this paper). The eigenpairs (\mathbf{f}, λ) that solve the generalized eigenvalue problem $\mathbf{A}\mathbf{f} = \lambda \mathbf{B}\mathbf{f}$ is an estimate to the eigensolutions of the Laplace-Beltrami operator.

Remark 2. In [18], the diagonal elements of \mathbf{S} are chosen in terms of the off-diagonals to ensure that the resulting problem has non-negative eigenvalues, as well as a trivial eigenvalue with corresponding eigenvector being constant. Since we aim to estimate operators that do not necessarily have such properties, we did not employ such an adjustment in our formulation and implementation. Moreover, explicit simplification of the integrals (14) and (13) can be found in [18] in the case of flat local meshes with the parameterization $\tilde{\Phi}_{T_{i,r}}$ in (3). We approximate the integral in the stiffness and mass matrices, \mathbf{S} and \mathbf{M} , with a first-order quadrature based on evaluating the nodes of the triangle T .

3.2 Generalization to operators on arbitrary tensor fields

For clarity, we first present the generalization of the framework from the previous subsection in terms of operators on vector fields when $d = 2$. However, this setup can be easily extended to estimate operators on arbitrary tensor fields over manifolds of higher dimension. First, one must introduce a new nodal basis. For vector fields, a natural choice is given in terms of the nodal basis for functions and the estimated tangent vectors by

$$\{e_i \mathbf{t}_\ell^{(i)}\}_{1 \leq i \leq N, 1 \leq \ell \leq d}. \quad (15)$$

In this case, any vector field $W : M \rightarrow TM$ can be expressed as,

$$W(x) = \sum_{i=1}^N \sum_{\ell=1}^d W_\ell^{(i)} e_i(x) \mathbf{t}_\ell^{(i)}.$$

Hence, the discrete approximation to eigenvalue problem $\langle DW, DW \rangle_U = \lambda \langle W, W \rangle_{T^{(1,0)}M}$, where the left-hand inner product is defined for appropriate range space of $D : T^{(1,0)}M \rightarrow U$ (e.g., $U = T^{(2,0)}M$ for Bochner Laplacian), is to solve the generalized eigenvalue problem,

$$\mathbf{A}\mathbf{W} = \lambda\mathbf{B}\mathbf{W}, \quad (16)$$

where λ denotes the eigenvalue corresponding to eigenvector field $\mathbf{W} \in \mathbb{R}^{Nd}$ with entries given by

$$\begin{pmatrix} (\mathbf{W})_{2i+1} \\ (\mathbf{W})_{2i+2} \end{pmatrix} = (\mathbf{t}_1^{(i)})^\top W(x_i) \mathbf{t}_1^{(i)} + (\mathbf{t}_2^{(i)})^\top W(x_i) \mathbf{t}_2^{(i)}$$

and $\mathbf{A} = \frac{1}{2}(\mathbf{S} + \mathbf{S}^\top)$ and $\mathbf{B} = \frac{1}{2}(\mathbf{M} + \mathbf{M}^\top)$ are the symmetrization of the stiffness and mass matrices \mathbf{A} and \mathbf{B} , respectively.

In this case, the mass and stiffness matrices are sparse, $dN \times dN$ matrices. It is convenient to define these matrices in terms of their $d \times d$ block submatrices. For $d = 2$, the mass matrix \mathbf{M} has 2×2 block entries given by,

$$\begin{bmatrix} [\mathbf{M}]_{2i-1,2j-1} & [\mathbf{M}]_{2i-1,2j} \\ [\mathbf{M}]_{2i,2j-1} & [\mathbf{M}]_{2i,2j} \end{bmatrix} = \sum_{T_{i,r} \in R(i)} \int_T e_i e_j \begin{bmatrix} \langle \mathbf{t}_1^{(i)}, \mathbf{t}_1^{(j)} \rangle_{g_{\Phi_{C_{i,r}}}} & \langle \mathbf{t}_1^{(i)}, \mathbf{t}_2^{(j)} \rangle_{g_{\Phi_{C_{i,r}}}} \\ \langle \mathbf{t}_2^{(i)}, \mathbf{t}_1^{(j)} \rangle_{g_{\Phi_{C_{i,r}}}} & \langle \mathbf{t}_2^{(i)}, \mathbf{t}_2^{(j)} \rangle_{g_{\Phi_{C_{i,r}}}} \end{bmatrix} \sqrt{\det(g_{\Phi_{C_{i,r}}})} du_1 du_2,$$

where the integrals above are taken entrywise, and the inner-products are Riemannian inner-products between vector fields. Also, we consider using the local curved mesh parameterization in the above since the flat local mesh parameterization introduces significant errors in the stiffness matrix calculation since the Christoffel symbols are all zero as we shall see below. Again, whenever $\{e_i\}_{i=1}^N$ are hat functions, the integrals simplify significantly, and many vanish. In particular, when $i \neq j$, the integrals vanish unless x_j is a neighbor of x_i (i.e., $x_j = x_i$ for some r) and $\bar{v}_i \bar{v}_i$ is a side in the triangulation of $R(i)$.

Define an arbitrary differential operator $D : TM \rightarrow \bigoplus_{r,s} T^{(r,s)}M$ acting on vector fields. For Bochner Laplacian, $D := \text{grad}_g : TM \rightarrow T^{(2,0)}M$ is gradient of vector field. For Hodge Laplacian, $D : TM \rightarrow T^{(2,0)}M \oplus C^\infty(M)$ defined as $D = (\nabla_g, d^\star \flat)$, where the first component is the gradient of vector field and d^\star in the second component denotes the codifferential of the exterior derivative, d , acting to 1-form, defined as, $d^\star = (-1)^{d-1} \text{sign}(g) \star d \star$, where $\star : \Omega^k(M) \rightarrow \Omega^{d-k}(M)$ is the standard Hodge star operator, and the musical notation \flat denotes the ‘‘lowering’’ operation that takes vector field to its covector field (1-form in our case). With this definition, we define the matrix \mathbf{S} with entries,

$$\begin{bmatrix} [\mathbf{S}]_{2i-1,2j-1} & [\mathbf{S}]_{2i-1,2j} \\ [\mathbf{S}]_{2i,2j-1} & [\mathbf{S}]_{2i,2j} \end{bmatrix} = \sum_{T_{i,r} \in R(i)} \int_T \begin{bmatrix} \langle De_i \mathbf{t}_1^{(i)}, De_j \mathbf{t}_1^{(j)} \rangle_{g_{\Phi_{C_{i,r}}}} & \langle De_i \mathbf{t}_1^{(i)}, De_j \mathbf{t}_2^{(j)} \rangle_{g_{\Phi_{C_{i,r}}}} \\ \langle De_i \mathbf{t}_2^{(i)}, De_j \mathbf{t}_1^{(j)} \rangle_{g_{\Phi_{C_{i,r}}}} & \langle De_i \mathbf{t}_2^{(i)}, De_j \mathbf{t}_2^{(j)} \rangle_{g_{\Phi_{C_{i,r}}}} \end{bmatrix} \sqrt{\det(g_{\Phi_{C_{i,r}}})} du_1 du_2,$$

where the Riemannian inner product operation in each component will be defined according to the codomain of D . In the case of Bochner Laplacian, the Riemannian inner product is over $(2,0)$ tensor field, whereas for the Hodge Laplacian, it will be defined over $(2,0)$ tensor fields and functions for the first and second components of the co-domain, respectively.

Detailed computations for the mass matrix for vector fields, as well as for the stiffness matrices for the Bochner and Hodge Laplacians in the case of the local curved mesh method are provided in the Appendices A.1, A.2, and A.3, respectively. Remaining details for computing the mass matrix are summarized in the following remark.

Remark 3. A subtlety in the above block formula is in computing $\langle \mathbf{t}_{k_1}^{(i)}, \mathbf{t}_{k_2}^{(j)} \rangle_{g_{\Phi_{C_{i,r}}}}$. Since the local parameterizations of these pair of tangent vectors are different, the former, $\Phi_{C_{i,r}}$, is constructed at base point x_i , whereas the latter, $\Phi_{C_{j,r}}$ is constructed at base point x_j , we need to represent these two vectors with the same coordinates to have a well defined inner product. To accomplish this, we first represent $\mathbf{t}_{k_2}^{(j)}$ in terms of $\{\mathbf{t}_1^{(i)}, \dots, \mathbf{t}_n^{(i)}\}$:

$$\mathbf{t}_{k_2}^{(j)} = \sum_{k=1}^n b_k \mathbf{t}_k^{(i)}$$

Let $\vec{b} = (b_1, \dots, b_n)^\top$. Similarly, let \vec{a} denote a vector of all zeros with a one in the k_1 -th position, which is the analogous representation for $\mathbf{t}_{k_1}^{(i)}$. We then regress the above vectors onto the natural basis for the tangent space corresponding to the parameterization, given by $\{\partial_{u_1} \Phi_{C_{i,r}}, \partial_{u_2} \Phi_{C_{i,r}}\}$ to obtain coefficient vector $\mathbf{a}_{k_1}^{ii}, \mathbf{a}_{k_2}^{ij}$ satisfying

$$\begin{aligned} \vec{a} &\approx (\mathbf{a}_{k_1}^{ii})_1 \partial_{u_1} \Phi_{C_{i,r}} + (\mathbf{a}_{k_1}^{ii})_2 \partial_{u_2} \Phi_{C_{i,r}} \\ \vec{b} &\approx (\mathbf{a}_{k_2}^{ij})_1 \partial_{u_1} \Phi_{C_{i,r}} + (\mathbf{a}_{k_2}^{ij})_2 \partial_{u_2} \Phi_{C_{i,r}} \end{aligned} \quad (17)$$

We can summarize the regression and coordinate transformation above compactly as,

$$\mathbf{a}_k^{ij} = \mathbf{R}_{i,r}^{LS} \mathbf{T}^\top \mathbf{t}_k^{(j)},$$

where $\mathbf{T} = [\mathbf{t}_1^{(i)}, \dots, \mathbf{t}_n^{(i)}] \in \mathbb{R}^{n \times n}$ and $\mathbf{R}_{i,r}^{LS} = (\mathbf{R}_{i,r}^\top \mathbf{R}_{i,r})^{-1} \mathbf{R}_{i,r}^\top$ is the least-squares operator corresponding to (17), where we have defined the matrix $\mathbf{R}_{i,r} = [\partial_{u_1}, \partial_{u_2}]$ whose columns form a tangent space for the local curved mesh of triangle $T_{i,r}$, as defined in (11). Thus, it is clear that

$$\langle \mathbf{t}_a^{(i)}, \mathbf{t}_b^{(j)} \rangle_{g_{\Phi_{C_{i,r}}}} = (\mathbf{a}_{k_1}^{ii})^\top g_{\Phi_{C_{i,r}}} \mathbf{a}_{k_2}^{ij}. \quad (18)$$

4 Convergence of Eigenvalues

In this section, we prove the convergence of eigenvalues of a Bochner Laplacian discretization (using the local curved mesh method), obtained from the generalized eigenvalue problem (16), to the true eigenvalues of the Bochner Laplacian. The proof hinges on weak consistency results of the form

$$|\langle \nabla W, \nabla W \rangle_{L^2(T^{(2,0)M})} - \langle \mathbf{D}^{-1} \mathbf{S} \mathbf{W}, \mathbf{W} \rangle| \longrightarrow 0 \text{ as } N \rightarrow \infty, \quad (19)$$

$$|\langle W, W \rangle_{L^2(T^{(1,0)M})} - \langle \mathbf{D}^{-1} \mathbf{M} \mathbf{W}, \mathbf{W} \rangle| \longrightarrow 0 \text{ as } N \rightarrow \infty, \quad (20)$$

where ∇ denotes the gradient on vector fields, W denotes a vector-field, \mathbf{W} denotes the vector field W evaluated on X , and \mathbf{D} denotes a diagonal normalization matrix which is defined in Section 4.3. With such a result in hand, the proof follows established arguments which leverage the min-max formula for the ℓ -th eigenvalue of the Bochner Laplacian:

$$\lambda_\ell = \min_{S \in \mathcal{G}_\ell} \max_{W \in S} \frac{\langle \nabla W, \nabla W \rangle_{L^2(T^{(2,0)M})}}{\langle W, W \rangle_{L^2(T^{(1,0)M})}} \quad (21)$$

where \mathcal{G}_ℓ denotes all smooth subspaces of vector-fields of dimension ℓ . We remark that the results of (19), (20) are sufficient to prove the convergence of eigenvalues of (16) due to the fact that the weak form $\min_{S_\ell \in \mathcal{G}_\ell} \max_{W \in S_\ell} \frac{\langle \mathbf{D}^{-1} \mathbf{S} \mathbf{W}, \mathbf{W} \rangle}{\langle \mathbf{D}^{-1} \mathbf{M} \mathbf{W}, \mathbf{W} \rangle}$ coincides with $\min_{S_\ell \in \mathcal{G}_\ell} \max_{W \in S_\ell} \frac{\langle \mathbf{A} \mathbf{W}, \mathbf{W} \rangle}{\langle \mathbf{B} \mathbf{W}, \mathbf{W} \rangle}$. For details, we refer the reader to Appendix B.

The rest of this section is organized as follows. In Section 4.1, we introduce some geometric preliminaries and define local charts which serve as the analytic object that is estimated by the local curved mesh method. We also state convergence results that follow from standard GMLS results adapted to our setup. In Section 4.2, we quantify the error that occurs in estimating vector fields using the nodal basis in (15). In Section 4.3, we patch local consistency results from Sections 4.2 and 4.1 together to prove a weak consistency formula of the form (19), from which the convergence of eigenvalues follows.

Throughout this section, we let $X = \{x_1, \dots, x_N\}$ denote a dataset of N points sampled uniformly from a manifold M . We remark that, for simplicity, we assume that the estimated tangent space $\overline{T_{x_i} M}$ is exact for each point i . In practice, high-order approximations of the tangent space can be obtained, and other error terms investigated in this analysis dominate. As in previous sections, we assume that the manifold is of dimension $d = 2$ embedded in \mathbb{R}^3 to simplify computations. However, generalizing the computations of this section to higher dimensional manifolds of higher codimension is straightforward.

4.1 Local metric approximation

Fix a point x_i and consider its k -nearest neighbors $K(i) = \{x_{i_1}, \dots, x_{i_k}\}$, as well as $T(i)$, which is $K(i)$ projected to $T_{x_i} M$. Let $R_i = \max_{\tilde{v}_j \in T(i)} \|\tilde{v}_j\|$. In the previous equation, and the remainder of this paper, $\|\cdot\|$ denotes the Euclidean norm (specifically, for vector in \mathbb{R}^d in the above). We remark that $k(N)$ is chosen to scale sufficiently slowly so that $R_i \rightarrow 0$. To this end, we assume that N is sufficiently large so that $R_i \leq r_M$, where r_M denotes the injectivity radius of the manifold.

To facilitate the analysis below, we define the local fill and separation distances, respectively:

$$h_i := \sup_{\tilde{v} \in B_0^d(R_i)} \min_{\tilde{v}_j \in T(i)} \|\tilde{v} - \tilde{v}_j\|, \quad q_X := \frac{1}{2} \min_{\tilde{v}_i, \tilde{v}_j \in T(i), i \neq j} \|\tilde{v}_i - \tilde{v}_j\|.$$

Consider also the global fill and separation distances, respectively:

$$h_{X,M} := \sup_{x \in M} \min_{x_j \in X} \|x - x_j\|, \quad q_i := \frac{1}{2} \min_{x_i, x_j \in T(i), i \neq j} \|x_i - x_j\|.$$

We assume that the dataset X is quasi-uniform in the sense that

$$q_X \leq h_{X,M} \leq c_q q_X, \quad (22)$$

for some constant c_q . It is easy to see that the projected data is also quasi-uniform same sense (i.e., that $q_i \leq h_i \leq c_{q_i} q_i$, for some constant $c_{q_i} > 0$). Since the points $\bar{v} \in B_{\bar{0}}(R_i)$ correspond to projected points in M , one can verify that

$$h_i \leq h_{X,M} \quad \text{for all } i \in \{1, \dots, N\}. \quad (23)$$

Let $\gamma_{x_i} : B_{\bar{0}}(R_i) \rightarrow \mathbb{R}^n$ denote a local parameterization of the form

$$\gamma_{x_i} : (v_1, v_2) \mapsto x_i + (v_1, v_2, z_{x_i}(v_1, v_2)), \quad (24)$$

for some smooth map z_{x_i} , which is obtained by projecting points nearby x_i to $T_{x_i}M$.

In this section, we quantify the error of estimating the coordinates induced by γ_{x_i} with the coordinates corresponding to α_{x_i} of (8). Such a result follows from general approximation error results from the GMLS, which have been derived in [24]. We state their results in our context below.

Lemma 4.1. *Let $X \subseteq M$ be such that $h_{X,M} \leq h_0$ for some constant $h_0 > 0$. Define $\Omega_i^* = \bigcup_{\bar{v} \in B_{\bar{0}}(R_i)} B_{\bar{v}}(C_2 h_0)$ for some constant $C_2 > 0$. Then for any $f \in C^{m+1}(\Omega_i^*)$, and α that satisfies $|\ell| \leq m$, we have*

$$|D^\ell f(\bar{v}) - D^\ell p_f(\bar{v})| \leq C h_i^{m+1-|\ell|} |f|_{C^{m+1}(\Omega_i^*)} \leq C h_{X,M}^{m+1-|\ell|} |f|_{C^{m+1}(\Omega_i^*)}$$

for any $\bar{v} \in B_{\bar{0}}(R_i)$ and multi-index ℓ with $|\ell| \leq m$.

In our case, we estimate the $d = 2$ dimensional smooth function z_{x_i} with polynomials of degree $m = 2$ such that,

$$\left| D^\ell z_{x_i}(\bar{v}) - D^\ell p_i(\bar{v}) \right| = O\left(h_{X,M}^{3-|\ell|}\right) \quad (25)$$

for any multi-index ℓ with $|\ell| \leq 2$. We remark that since $z_{x_i} : B_{\bar{0}}(R_i) \rightarrow \mathbb{R}^n$ is smooth, it can certainly be extended to a smooth function on Ω_i^* .

Using this result, we can obtain bounds on estimating the necessary local quantities. The proof is simple, and can be found in Appendix B.

Lemma 4.2. *Denote by $\{\partial_{v_1}(\gamma_{x_i}), \partial_{v_2}(\gamma_{x_i})\}$ and $\{\partial_{v_1}(\alpha_{x_i}), \partial_{v_2}(\alpha_{x_i})\}$ the coordinates induced from γ_{x_i} and α_{x_i} respectively. Denote the Riemannian metric associated with each set of coordinates by $g_{\gamma_{x_i}}$ and $g_{\alpha_{x_i}}$, and the components of their inverse as $g_{\gamma_{x_i}}^{qs}$ and $g_{\alpha_{x_i}}^{qs}$. Let $\Gamma_{st}^q(\gamma_{x_i}), \Gamma_{st}^q(\alpha_{x_i})$ denote the Christoffel symbols associated with $g_{\gamma_{x_i}}, g_{\alpha_{x_i}}$, respectively. Fix any triangle $T_{i,r} \in R(i)$. Then for any $\bar{v} \in T_{i,r}$,*

$$\begin{aligned} \|\partial_{v_k}(\gamma_{x_i})(\bar{v}) - \partial_{v_k}(\alpha_{x_i})(\bar{v})\| &= O(h_{X,M}^2), \quad k = 1, 2 \\ \left| \sqrt{\det(g_{\gamma_{x_i}})(\bar{v})} - \sqrt{\det(g_{\alpha_{x_i}})(\bar{v})} \right| &= O(h_{X,M}) \\ \left| \left(g_{\gamma_{x_i}}^{qs} \right)(\bar{v}) - \left(g_{\alpha_{x_i}}^{qs} \right)(\bar{v}) \right| &= O(h_{X,M}) \\ \left| \Gamma_{st}^q(\gamma_{x_i})(\bar{v}) - \Gamma_{st}^q(\alpha_{x_i})(\bar{v}) \right| &= O(h_{X,M}). \end{aligned}$$

4.2 Local vector field approximation

The results of the previous subsection quantify the error between estimating the metric and its derivatives. What remains for obtaining error bounds on the estimation of the local integral formula for the Bochner Laplacian is to quantify the error coming from the estimation of a vector-field W using the nodal basis. To this end, consider a vector field $W : M \rightarrow TM$. While the computation is done via the representation of the vector field under the basis $\{\partial_{u_1} \Phi_{C_{i,r}}, \partial_{u_2} \Phi_{C_{i,r}}\}$ evaluated at $(\Phi_{i,r})^{-1}(\bar{v}_{i,r})$ as discussed in Remark 3, it is theoretically more convenient to work in the tangent space $T_{x_i}M$, leveraging the error bounds induced by the estimated coordinate system $\{\partial_{v_1}(\alpha_{x_i}), \partial_{v_2}(\alpha_{x_i})\}$ as deduced in Lemma 4.2. Analytically, due to the diffeomorphism outlined in Section 4.1, any vector field $W : M \rightarrow TM$ can be written in the local coordinates as

$$W(v_1, v_2) = c_1^{(i,r)}(v_1, v_2) \partial_{v_1}(\gamma_{x_i}) + c_2^{(i,r)}(v_1, v_2) \partial_{v_2}(\gamma_{x_i}).$$

Numerically, we estimate W on $T_{i,r}$ by:

$$\widehat{W}(v_1, v_2) = \widehat{b}_1^{(i,r)}(v_1, v_2) \partial_{v_1}(\alpha_{x_i}) + \widehat{b}_2^{(i,r)}(v_1, v_2) \partial_{v_2}(\alpha_{x_i}) \quad (26)$$

where the estimated coefficients, which are functions of $T_{i,r}$, are denoted by $\{\widehat{b}_k^{(i,r)}\}_{k=1,2}$.

In the following lemma, we estimate the error $\|(D^\alpha W)(v_1, v_2) - (D^\alpha \widehat{W})(v_1, v_2)\|$. Intuitively, this can be broken down into two parts: coefficient function error (coming from estimation of the smooth coefficient functions using the nodal basis), and basis approximation error (i.e., between $\partial_{v_k}(\gamma_{x_i})$ and $\partial_{v_k}(\alpha_{x_i})$). The former is bounded using standard results in the finite element literature, as well as standard perturbation theory for linear regression, while the latter error is quantified in Section 4.1.

Lemma 4.3. *Let $W : M \rightarrow TM$ be a C^2 vector field. For a given $x_i \in X$, consider any triangle $T_{i,r} \in R(i)$, and fix any $(v_1, v_2) \in T_{i,r}$. Denote by $W(v_1, v_2)$ a local representation of W in the analytic charts induced by γ_{x_i} . Let $\widehat{W}(v_1, v_2)$ denote the estimation defined in (26), where the parameterizations $\{\alpha_{x_i}\}_{i=1}^N$ are estimated using polynomials of degree 2 as in (6). Then*

$$\|D^\ell W(v_1, v_2) - D^\ell \widehat{W}(v_1, v_2)\| = O(h_{X,M}), \quad (27)$$

where $h_{X,M}$ is the global fill distance defined as before and ℓ is an index of order $|\ell| \leq 1$, where the constant depends on the local separation distance q_i .

Proof. Fix $(v_1, v_2) \in T_{i,r}$. Recall that

$$\begin{aligned} \widehat{W}(v_1, v_2) &= \widehat{b}_1^{(i,r)}(v_1, v_2) \partial_{v_1}(\alpha_{x_i})(v_1, v_2) + \widehat{b}_2^{(i,r)}(v_1, v_2) \partial_{v_2}(\alpha_{x_i})(v_1, v_2) \\ W(v_1, v_2) &= c_1^{(i,r)}(v_1, v_2) \partial_{v_1}(\gamma_{x_i})(v_1, v_2) + c_2^{(i,r)}(v_1, v_2) \partial_{v_2}(\gamma_{x_i})(v_1, v_2). \end{aligned}$$

We introduce two intermediate estimators:

$$\begin{aligned} \overline{W}(v_1, v_2) &= \widehat{c}_1^{(i,r)}(v_1, v_2) \partial_{v_1}(\alpha_{x_i})(v_1, v_2) + \widehat{c}_2^{(i,r)}(v_1, v_2) \partial_{v_2}(\alpha_{x_i})(v_1, v_2) \\ \widetilde{W}(v_1, v_2) &= \widehat{c}_1^{(i,r)}(v_1, v_2) \partial_{v_1}(\gamma_{x_i})(v_1, v_2) + \widehat{c}_2^{(i,r)}(v_1, v_2) \partial_{v_2}(\gamma_{x_i})(v_1, v_2), \end{aligned}$$

where $\widehat{c}_k^{(i,r)}$ is an interpolation of $c_k^{(i,r)}$ using nodal basis functions and the values of on the vertices of $T_{i,r}$. We split the error as follows:

$$\begin{aligned} \|D^\ell W(v_1, v_2) - D^\ell \widehat{W}(v_1, v_2)\| &\leq \|D^\ell W(v_1, v_2) - D^\ell \widetilde{W}(v_1, v_2)\| + \|D^\ell \widetilde{W}(v_1, v_2) - D^\ell \overline{W}(v_1, v_2)\| \\ &\quad + \|D^\ell \overline{W}(v_1, v_2) - D^\ell \widehat{W}(v_1, v_2)\|. \end{aligned}$$

The error of the first term can be analyzed in the basis of the ambient space:

$$\begin{aligned} \|D^\ell W(v_1, v_2) - D^\ell \widetilde{W}(v_1, v_2)\| &= \left\| \sum_{j=1}^n \left((D^\ell W(v_1, v_2) - D^\ell \widetilde{W}(v_1, v_2)) \cdot \mathbf{e}_j \right) \mathbf{e}_j \right\| \\ &= \sqrt{\sum_{j=1}^n \left(\sum_{k=1}^d D^\ell (\widehat{c}_k^{i,r} - c_k^{i,r}) \partial_{v_k}(\gamma_{x_i}) \cdot \mathbf{e}_j + (\widehat{c}_k^{i,r} - c_k^{i,r}) D^\ell \partial_{v_k}(\gamma_{x_i}) \cdot \mathbf{e}_j \right)^2}. \end{aligned}$$

For simplicity of notation, we have suppressed the evaluation on (v_1, v_2) above, as we do in what follows. We note that, for quasi-uniform data, we have $h_i/q_i \leq c_{q_i}$. Consider the following standard finite element result. For any polynomial of degree $m-1$ interpolant \widehat{f} of a function $f \in W^{m,p}(T_{i,r})$, we have the following local interpolation error bound (see e.g. Theorem 4.4.4, in [7]):

$$|\widehat{f} - f|_{W^{\ell,p}(T_{i,r})} \leq c h_i^{m-\ell} q_i^\ell |f|_{W^{m,p}(T_{i,r})}$$

$1 \leq p \leq \infty, 0 \leq \ell \leq m$. It follows that, for $m=2, p=\infty$, we have,

$$\left| \widehat{c}_k^{i,r} - c_k^{i,r} \right|_{W^{1,\infty}(T_{i,r})} = O(h_i), \quad \left| \widehat{c}_k^{i,r} - c_k^{i,r} \right|_{L^\infty(T_{i,r})} = O(h_i^2).$$

Hence,

$$\|D^\ell W(v_1, v_2) - D^\ell \widetilde{W}(v_1, v_2)\| = O(h_i).$$

For the term $\|D^\ell \widetilde{W}(v_1, v_2) - D^\ell \overline{W}(v_1, v_2)\|$, we again analyze the error in the basis of the ambient space:

$$\begin{aligned} \|D^\ell \widetilde{W}(v_1, v_2) - D^\ell \overline{W}(v_1, v_2)\| &= \left\| \sum_{j=1}^n \left((D^\ell \widetilde{W}(v_1, v_2) - D^\ell \overline{W}(v_1, v_2)) \cdot \mathbf{e}_j \right) \mathbf{e}_j \right\| \\ &= \sqrt{\sum_{j=1}^n \left(\sum_{k=1}^d (D^\ell \widehat{c}_k^{i,r}) (\partial_{v_k}(\gamma_{x_i}) - \partial_{v_k}(\alpha_{x_i})) \cdot \mathbf{e}_j + \widehat{c}_k^{i,r} D^\ell (\partial_{v_k}(\gamma_{x_i}) - \partial_{v_k}(\alpha_{x_i})) \cdot \mathbf{e}_j \right)^2}. \end{aligned}$$

We proved in Lemma 4.2 that $\|D^\ell(\partial_{v_k}(\gamma_{x_i}) - \partial_{v_k}(\alpha_{x_i}))\| = O(h_i^{2-\ell})$ for $\ell = 0, 1$. Hence,

$$\|D^\ell \widetilde{W}(v_1, v_2) - D^\ell \overline{W}(v_1, v_2)\| = O(h_i).$$

Now, it only remains to bound $\|D^\ell \overline{W}(v_1, v_2) - D^\ell \widehat{W}(v_1, v_2)\|$. For this, writing in the ambient space basis, we have:

$$\begin{aligned} \|D^\ell \overline{W}(v_1, v_2) - D^\ell \widehat{W}(v_1, v_2)\| &= \left\| \sum_{j=1}^n \left((D^\ell \overline{W}(v_1, v_2) - D^\ell \widehat{W}(v_1, v_2)) \cdot \mathbf{e}_j \right) \mathbf{e}_j \right\| \\ &= \sqrt{\sum_{j=1}^n \left(\sum_{k=1}^d D^\ell (\widehat{c}_k^{i,r} - \widehat{b}_k^{i,r}) \partial_{v_k}(\alpha_{x_i}) \cdot \mathbf{e}_j + (\widehat{c}_k^{i,r} - \widehat{b}_k^{i,r}) D^\ell \partial_{v_k}(\alpha_{x_i}) \cdot \mathbf{e}_j \right)^2}. \end{aligned}$$

Clearly, it suffices to bound $|D^\ell(\widehat{c}_k^{i,r} - \widehat{b}_k^{i,r})|$. Recall that $\widehat{c}_k^{i,r}$ is interpolated by hat functions based on the values $u(x_i), u(x_{i_{j_r}}), u(x_{i_{k_r}})$ written in the basis $\{\partial_{v_1}(\gamma_{x_i}), \partial_{v_2}(\gamma_{x_i})\}$. Similarly for $\widehat{b}_k^{i,r}$, but in the basis $\{\partial_{v_1}(\alpha_{x_i}), \partial_{v_2}(\alpha_{x_i})\}$.

Let $\tilde{v}_{i_{j_r}}$ denote an arbitrary vertex in $T_{i,r}$. Define the following:

$$\begin{aligned} \mathbf{C} &= \begin{bmatrix} \partial_{v_1}(\gamma_{x_i})(\tilde{v}_{i_{j_r}}), \partial_{v_2}(\gamma_{x_i})(\tilde{v}_{i_{j_r}}) \end{bmatrix}, & \mathbf{D} &= \begin{bmatrix} \partial_{v_1}(\alpha_{x_i})(\tilde{v}_{i_{j_r}}), \partial_{v_2}(\alpha_{x_i})(\tilde{v}_{i_{j_r}}) \end{bmatrix}, \\ \widehat{\mathbf{c}} &= \left(\widehat{c}_1^{i,r}(\tilde{v}_{i_{j_r}}), \widehat{c}_2^{i,r}(\tilde{v}_{i_{j_r}}) \right)^\top, & \widehat{\mathbf{b}} &= \left(\widehat{b}_1^{i,r}(\tilde{v}_{i_{j_r}}), \widehat{b}_2^{i,r}(\tilde{v}_{i_{j_r}}) \right)^\top. \end{aligned}$$

We remark that $W(\tilde{v}_{i_{j_r}}) = \mathbf{C}\widehat{\mathbf{c}}$, and $W(\tilde{v}_{i_{j_r}}) = \mathbf{D}\widehat{\mathbf{b}} + \widehat{\mathbf{r}}$, where the first regression problem has no residual as $\widehat{\mathbf{c}} = \mathbf{c}$ on the vertex of the $T_{i,r}$, whereas the second regression problem may have a residual due to the approximation of the basis representation. Since $\|\partial_{v_k}(\gamma_{x_i}) - \partial_{v_k}(\alpha_{x_i})\| = O(h_i)$, it follows that $\|\mathbf{D} - \mathbf{C}\|_2 \leq \|\mathbf{D} - \mathbf{C}\|_F = O(h_i)$, where $\|\cdot\|_2$ and $\|\cdot\|_F$ denote the spectral and Frobenius matrix norms, respectively. Since the condition number of $\kappa_2(\mathbf{C}) = O(1)$, for any small perturbation $h_i \ll 1$, it follows from standard least squares perturbation results (e.g., see Theorem 3.4 of [11]) that $\|\widehat{\mathbf{c}} - \widehat{\mathbf{b}}\| \leq h_i 2\kappa_2(\mathbf{C}) \|\widehat{\mathbf{c}}\|$. Hence,

$$|\widehat{b}_k^{i,r}(\tilde{v}_{i_{j_r}}) - \widehat{c}_k^{i,r}(\tilde{v}_{i_{j_r}})| = O(h_i).$$

Since $\tilde{v}_{i_{j_r}}$ is an arbitrary vertex of $T_{i,r}$, it follows immediately from definition of hat functions that

$$|D^\ell(\widehat{b}_k^{i,r}(v_1, v_2) - \widehat{c}_k^{i,r}(v_1, v_2))| = O(h_i), \quad \forall (v_1, v_2) \in T_{i,r}.$$

Finally, we remark that each above bound in h_i has a global bound in terms of $h_{X,M}$. This completes the proof. \square

4.3 Weak consistency

Fix a vector field $W : M \rightarrow TM$ and let \widehat{W} denote its estimation using the nodal basis for vector fields as defined in (26). In this subsection, we aim to quantify the error bound for,

$$\left| \int_M \langle \nabla W, \nabla W \rangle_g d\text{Vol} - \frac{1}{N} \langle \mathbf{D}^{-1} \mathbf{S} \mathbf{W}, \mathbf{W} \rangle \right|, \quad \text{and} \quad \left| \int_M \langle W, W \rangle_g d\text{Vol} - \frac{1}{N} \langle \mathbf{D}^{-1} \mathbf{M} \mathbf{W}, \mathbf{W} \rangle \right|. \quad (28)$$

In the above, \mathbf{D} denotes a diagonal matrix with entries $(\mathbf{D})_{d(i-1)+1, 2(i-1)+1}, \dots, (\mathbf{D})_{di, di} = \text{Vol}(R(i))$. By construction of the stiffness matrix, the term $\frac{1}{N} \langle \mathbf{D}^{-1} \mathbf{S} \mathbf{W}, \mathbf{W} \rangle$ corresponds to a discrete estimator of the Dirichlet energy. Namely,

$$\frac{1}{N} \langle \mathbf{D}^{-1} \mathbf{S} \mathbf{W}, \mathbf{W} \rangle = \sum_{i=1}^N \sum_{T_{i,r} \in R(i)} \frac{1}{\text{Vol}(R(i))N} \int_T \langle \nabla \widehat{W}, \nabla \widehat{W} \rangle_{g_{\Phi_{C_{i,r}}}} \sqrt{\det(g_{\Phi_{C_{i,r}}})} du_1 du_2,$$

where \widehat{W} corresponds to an interpolation of the discrete vector field \mathbf{W} using the nodal basis. Similarly,

$$\frac{1}{N} \langle \mathbf{D}^{-1} \mathbf{M} \mathbf{W}, \mathbf{W} \rangle = \sum_{i=1}^N \sum_{T_{i,r} \in R(i)} \frac{1}{\text{Vol}(R(i))N} \int_T \langle \widehat{W}, \widehat{W} \rangle_{g_{\Phi_{C_{i,r}}}} \sqrt{\det(g_{\Phi_{C_{i,r}}})} du_1 du_2.$$

By the previous discussion, the integrals in (28) can be written in the local coordinates arising from the parameterizations γ_{x_i} . Hence, the upper bounds for the differences in (28) include the errors of estimating $g_{\gamma_{x_i}}$, its inverse, and their derivatives, which is quantified in Section 4.1 and the local FEM error in estimating W and its derivatives, which is quantified in Section 4.2. Hence, with these error estimates, we will subsequently employ standard min-max arguments on the symmetrized discrete energy $\frac{\langle \mathbf{D}^{-1} \mathbf{S} \mathbf{W}, \mathbf{W} \rangle}{\langle \mathbf{D}^{-1} \mathbf{M} \mathbf{W}, \mathbf{W} \rangle}$ to establish the spectral error estimate.

The following local integration convergence result follows immediately from Lemmas 4.2 and 4.3. Its proof can be found in Appendix B

Lemma 4.4. Denote by W a vector field $W : M \rightarrow TM$. Let $(\nabla W)_{\gamma_{x_i}}$ be the local formula for the Bochner Laplacian on a vector field in the coordinates γ_{x_i} :

$$(\nabla W)_{\gamma_{x_i}} := g_{\gamma_{x_i}}^{sj} \left(\frac{\partial W^t}{\partial v_s} + W^p \Gamma_{ps}^t(\gamma_{x_i}) \right) \frac{\partial}{\partial v_t} \otimes \frac{\partial}{\partial v_j}.$$

Similarly,

$$(\nabla \widehat{W})_{\alpha_{x_i}} := g_{\alpha_{x_i}}^{sj} \left(\frac{\partial \widehat{W}^t}{\partial v_s} + \widehat{W}^p \Gamma_{ps}^t(\alpha_{x_i}) \right) \frac{\partial}{\partial v_t} \otimes \frac{\partial}{\partial v_j}.$$

Then

$$\left| \int_{T_{i,r}} \left(\left\langle (\nabla W)_{\gamma_{x_i}}, (\nabla W)_{\gamma_{x_i}} \right\rangle_{g_{\gamma_{x_i}}} \sqrt{\det(g_{\gamma_{x_i}})} - \left\langle (\nabla \widehat{W})_{\alpha_{x_i}}, (\nabla \widehat{W})_{\alpha_{x_i}} \right\rangle_{g_{\alpha_{x_i}}} \sqrt{\det(g_{\alpha_{x_i}})} \right) dv_1 dv_2 \right| = O(\text{Vol}(T_{i,r}) h_{X,M}).$$

We are now ready to state and prove the primary result of this subsection.

Theorem 4.1 (Weak error bounds). Fix a smooth vector field $W \in \mathfrak{X}(M)$ and let \mathbf{W} be denote W restricted to X . Let X be quasi-uniform in the sense of (22). Then, for sufficiently large N , with probability higher than $1 - \frac{2}{N}$,

$$\left| \int_M \langle \nabla W, \nabla W \rangle_g d\text{Vol} - \frac{1}{N} \langle \mathbf{D}^{-1} \mathbf{S} \mathbf{W}, \mathbf{W} \rangle \right| = O(N^{-1/2}) + O(h_{X,M}). \quad (29)$$

Also, with probability higher than $1 - \frac{2}{N}$,

$$\left| \int_M \langle W, W \rangle_g d\text{Vol} - \frac{1}{N} \langle \mathbf{D}^{-1} \mathbf{M} \mathbf{W}, \mathbf{W} \rangle \right| = O(N^{-1/2}) + O(h_{X,M}). \quad (30)$$

Proof. Let \widehat{W} be the estimated vector field defined in (26). Recall that, by construction,

$$\begin{aligned} \frac{1}{N} \langle \mathbf{D}^{-1} \mathbf{S} \mathbf{W}, \mathbf{W} \rangle &= \sum_{i=1}^N \sum_{T_{i,r} \in R(i)} \frac{1}{\text{Vol}(R(i))N} \int_T \langle \nabla \widehat{W}, \nabla \widehat{W} \rangle_{g_{\Phi_{C_{i,r}}}} \sqrt{\det(g_{\Phi_{C_{i,r}}})} du_1 du_2, \\ \frac{1}{N} \langle \mathbf{D}^{-1} \mathbf{M} \mathbf{W}, \mathbf{W} \rangle &= \sum_{i=1}^N \sum_{T_{i,r} \in R(i)} \frac{1}{\text{Vol}(R(i))N} \int_T \langle \widehat{W}, \widehat{W} \rangle_{g_{\Phi_{C_{i,r}}}} \sqrt{\det(g_{\Phi_{C_{i,r}}})} du_1 du_2. \end{aligned}$$

In what follows, we only prove (29). One can verify (30) following the same argument below. Consider the analytic, local parameterizations $\{\gamma_{x_i}\}_{i=1}^N$. Recall that Hoeffding's inequality states that, for a random variable f , given that $|f(x) - \int_M f d\text{Vol}| \leq C$ for all $x \in M$, then for all $\epsilon > 0$, we have that with probability higher than $1 - 2e^{-\frac{N\epsilon^2}{2C^2}}$, $|\int_M f d\text{Vol} - \frac{1}{N} \sum_{i=1}^N f(x_i)| \leq \epsilon$. Choosing $\epsilon = \sqrt{\log(N)/N}$ and using the fact that W is smooth along with the local charts $\{\gamma_{x_i}\}_{i=1}^N$, it follows immediately from Hoeffding's inequality that with probability higher than $1 - \frac{2}{N}$,

$$\left| \int_M \langle \nabla W, \nabla W \rangle_g d\text{Vol} - \frac{1}{N} \sum_{i=1}^N \langle \nabla W, \nabla W \rangle_{g_{\gamma_{x_i}}}(\vec{0}) \sqrt{\det(g_{\gamma_{x_i}})}(\vec{0}) \right| = O(N^{-1/2}),$$

where the local quantities above are evaluated at the basepoint $\vec{0} \in T_{x_i}M$, and the constant depends on $\langle \nabla W, \nabla W \rangle_g$. By smoothness of the integrand and Taylor's expansion, one can verify that,

$$\left| \langle \nabla W, \nabla W \rangle_{g_{\gamma_{x_i}}}(\vec{0}) \sqrt{\det(g_{\gamma_{x_i}})}(\vec{0}) - \frac{1}{\text{Vol}(R(i))} \int_{R(i)} \langle \nabla W, \nabla W \rangle_{g_{\gamma_{x_i}}} \sqrt{\det(g_{\gamma_{x_i}})} \right| = O(h_{X,M}),$$

and hence

$$\left| \int_M \langle \nabla W, \nabla W \rangle_g d\text{Vol} - \frac{1}{N} \sum_{i=1}^N \frac{1}{\text{Vol}(R(i))} \int_{R(i)} \langle \nabla W, \nabla W \rangle_{g_{\gamma_{x_i}}} \sqrt{\det(g_{\gamma_{x_i}})} \right| = O(N^{-1/2}) + O(h_{X,M}).$$

From Lemma 4.4, we have that

$$\frac{1}{N} \sum_{i=1}^N \frac{1}{\text{Vol}(R(i))} \sum_{T_{i,r} \in R(i)} \int_{T_{i,r}} \left| \langle \nabla W, \nabla W \rangle_{g_{\gamma_{x_i}}} \sqrt{\det(g_{\gamma_{x_i}})} - \langle \nabla \widehat{W}, \nabla \widehat{W} \rangle_{g_{\alpha_{x_i}}} \sqrt{\det(g_{\alpha_{x_i}})} \right| = O(h_{X,M}).$$

Combining these two estimates above, we have that

$$\left| \int_M \langle \nabla W, \nabla W \rangle_g d\text{Vol} - \sum_{i=1}^N \sum_{T_{i,r} \in R(i)} \frac{1}{\text{Vol}(R(i))N} \int_{T_{i,r}} \langle \nabla \widehat{W}, \nabla \widehat{W} \rangle_{g_{\alpha_{x_i}}} \sqrt{\det(g_{\alpha_{x_i}})} \right| = O(N^{-1/2}) + O(h_{X,M}).$$

We can reparameterize the integrands of the right-most term via $\Phi_{i,r} : T \rightarrow T_{i,r}$:

$$\int_T \left\langle (\nabla \widehat{W})_{\Phi_{C_{i,r}}}, (\nabla \widehat{W})_{\Phi_{C_{i,r}}} \right\rangle_{g_{\Phi_{C_{i,r}}}} \sqrt{\det(g_{\Phi_{C_{i,r}}})} du_1 du_2 = \int_{T_{i,r}} \left\langle (\nabla \widehat{W})_{\alpha_{x_i}}, (\nabla \widehat{W})_{\alpha_{x_i}} \right\rangle_{g_{\alpha_{x_i}}} \sqrt{\det(g_{\alpha_{x_i}})} dv_1 dv_2.$$

The desired result follows immediately. \square

From the above results, the convergence of eigenvalues follows from standard arguments. The proof can be found in Appendix B.

Corollary 4.1 (Spectral error bound). *Let λ_ℓ denote the ℓ -th eigenvalue of the Bochner Laplacian. Let λ_ℓ^N denote the ℓ -th eigenvalue corresponding to eigenvector field \mathbf{v} of the generalized eigenvalue problem:*

$$\mathbf{A}\mathbf{v} = \lambda_\ell^N \mathbf{B}\mathbf{v}. \quad (28)$$

For sufficiently large N , we have that with probability higher than $1 - \frac{8}{N}$,

$$|\lambda_\ell - \lambda_\ell^N| = O(N^{-1/2}) + O(h_{X,M}).$$

5 Numerical Results

In this section, we numerically implement the local curved mesh method estimation of the Bochner and Hodge Laplacians on some example manifolds. In this study, we numerically demonstrate the convergence of eigenvalues and eigenvectors of the generalized eigenvalue problem in (16) obtained from randomly sampled data to the analytic eigenvalues and eigenvector fields of the Bochner and Hodge Laplacians on the 2D sphere and the latter on a 2D torus. In Section 5.1, we demonstrate the convergence of eigenvalues and eigenvector fields for both the Hodge and Bochner Laplacian on the sphere, since the analytic eigenvalues and eigenvector-fields are known. Since analytic eigensolutions for the Bochner and Hodge Laplacian on a torus are unknown, we demonstrate the convergence of eigenvalues of the estimated Hodge Laplacian to semi-analytic solutions in Section 5.2. Finally, since in practical situations, one often has access to noisy observations that do not lie precisely on a manifold, we numerically investigate the robustness of this algorithm to noise in Section 5.3. For convenience, we refer to the estimations obtained from the curved mesh method by CMM.

5.1 Bochner and Hodge Laplacian Estimations on Sphere

In this section, we demonstrate the numerical convergence of the Hodge and Bochner Laplacians on the 2D unit sphere, $M = \{x \in \mathbb{R}^3 : \|x\| = 1\}$, embedded in \mathbb{R}^3 . To simulate uniform random sampling on this surface, we take the following approach: first, we generate a vector in \mathbb{R}^3 via $\tilde{w}_i \sim \mathcal{N}(\mathbf{0}, \mathbf{I})$. We then normalize each sample: $x_i = \tilde{w}_i / \|\tilde{w}_i\|$. An example of the resulting dataset is shown in Figure 1a.

Analytic eigensolutions for the Bochner and Hodge Laplacians on this manifold are well known. For a detailed description, see, for instance Section 5.4 of [16]. To summarize, the distinct eigenvalues of the Hodge and Bochner are given by the following:

$$\begin{aligned} \text{Hodge: } \lambda_\ell &= (\ell + 1)\ell, \\ \text{Bochner: } \lambda_\ell &= (\ell + 1)\ell - 1, \quad \ell \in \mathbb{N}^+. \end{aligned}$$

Since the sphere is of constant curvature, the Hodge and Bochner Laplacians share eigenvector fields. Eigenvector fields for the first 3 distinct eigenspaces are given by $\{\mathbf{n} \times \nabla_{\mathbb{R}^3} f, \mathbf{P}\nabla_{\mathbb{R}^3} f\}$, where \mathbf{n} denotes the outward facing normal vector, \mathbf{P} denotes the tangential projection tensor projecting $(\nabla_{\mathbb{R}^3} f)(x)$ to $T_x M$, and f is given by one of the spherical harmonics:

$$\begin{aligned} f(\vec{v}) &= (\vec{v})_i, \quad \text{for } \ell = 1, \\ f(\vec{v}) &= 3(\vec{v})_i(\vec{v})_k - \delta_{ik}, \quad \text{for } \ell = 2, \\ f(\vec{v}) &= 15(\vec{v})_i(\vec{v})_j(\vec{v})_k - 3\delta_{ij}(\vec{v})_k - 3\delta_{ki}(\vec{v})_j - 3\delta_{jk}(\vec{v})_i, \quad \text{for } \ell = 3, \end{aligned}$$

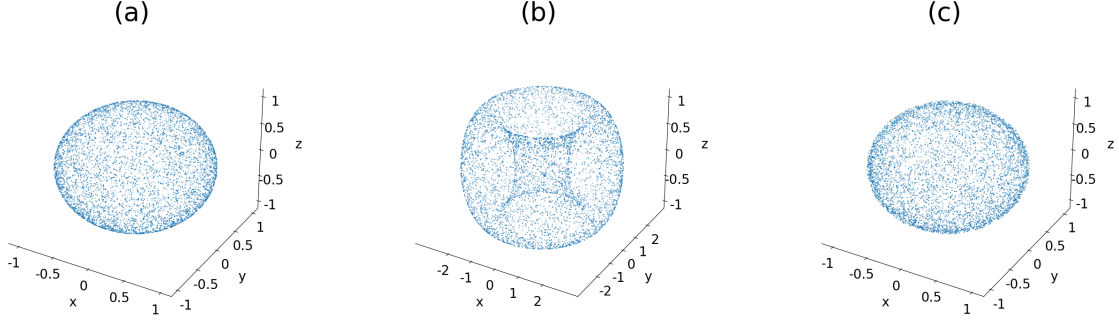


Figure 1: Example datasets used for numerical experiments. Displayed is a single trial with $N = 4000$ points for (a) sphere (b) torus, and (c) noisy sphere (each data point is perturbed in the normal direction with uniform noise of size 0.10).

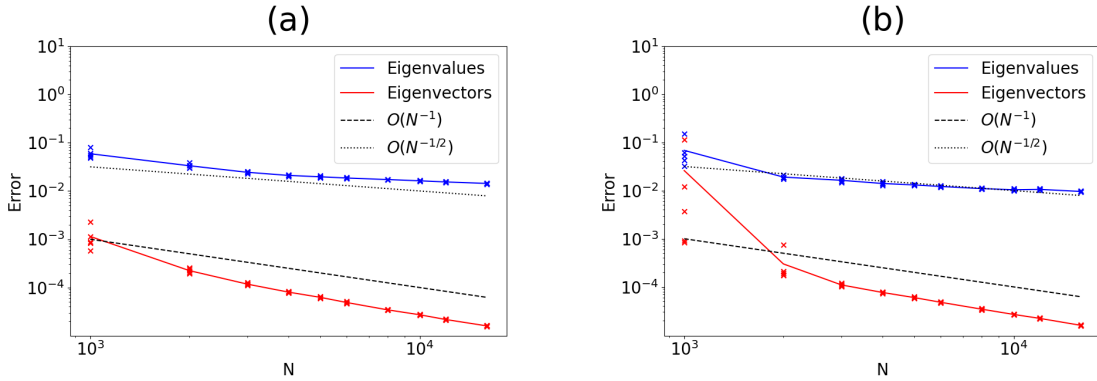


Figure 2: Operator estimation on sphere with uniform sampling distribution. Average of relative error (eigenvalues, leading $L = 48$ modes) and Average of mean-square-error (eigenvectors, leading $L = 6$ modes) as defined in Equation (29), (30) respectively: (a) Bochner Laplacian; (b) Hodge Laplacian.

where $i, j, k \in \{1, 2, 3\}$. We remark that the above formulas imply the dimension of the first three eigenspaces, where color indicates pointwise vector norm.

Figure 2 displays the convergence of CMM for the estimation of eigenvalues and eigenvector fields of the Bochner and Hodge Laplacians as functions of N . The error metrics reported for convergence are given by

$$\text{Error of eigenvalues} := \frac{1}{L} \sum_{j=1}^L \frac{|\lambda_j - \lambda_j^N|}{\lambda_j} \quad (29)$$

$$\text{Error of eigenvector fields} := \frac{1}{NL} \sum_{i=1}^N \sum_{j=1}^L \left\| W^{(j)}(x_i) - \widehat{W}^{(j)}(x_i) \right\|^2, \quad (30)$$

where $W^{(j)}(x_i)$ denotes the j -th analytic vector field described above, and $\widehat{W}^{(j)}$ denotes the least-squares linear combination of eigenvectors of the CMM estimator associated with the corresponding estimated eigenspace. We note that the above enumeration of eigenvalues is not distinct (i.e., includes multiplicities). In Figure 2a, results for estimating the Bochner Laplacian are shown, while in Figure 2b the corresponding results for the Hodge Laplacian are shown. We remark that, in either case, Corollary 4.1 is verified with a convergence rate of $O(N^{-1/d})$. In particular, one can show (see Appendix B, Lemma B.2 of [16]) that as $N \rightarrow \infty$, $h_{X,M} = O(N^{-1/d})$ almost surely. We remark that, since $d = 2$, this rate coincides with the Monte-Carlo rate. We also note that, for sufficiently large N , variance of eigenvalue computations for different samples of random data is minimal, which is desirable. For visual comparison, Figure 3 shows estimations (CMM estimation of Bochner Laplacian) of the first 4 eigenvector fields from a single trial with $N = 6000$. Overall, this example demonstrates that CMM can be used to accurately approximate multiple operators acting on vector fields, with competitive convergence rates.

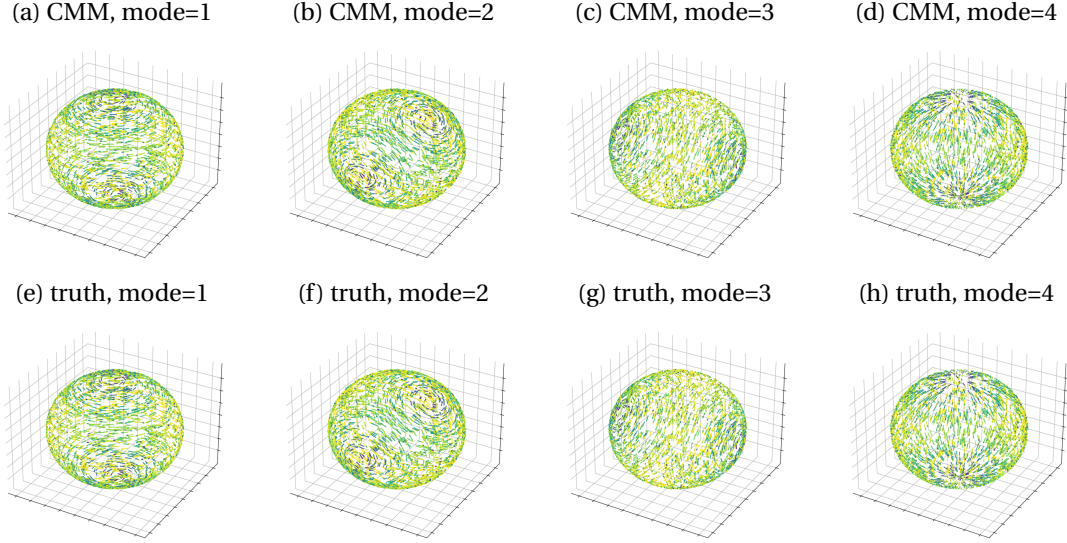


Figure 3: Visual comparison of the first four eigenvector fields for the Bochner Laplacian obtained using CMM (row 1) and analytic methods (row 2). The estimates are obtained from a single trial of $N = 6000$ randomly sampled points. Color indicates vector norm. Vectors visualized correspond to on a random subset of size 2000.

5.2 Hodge Laplacian Estimation on Torus

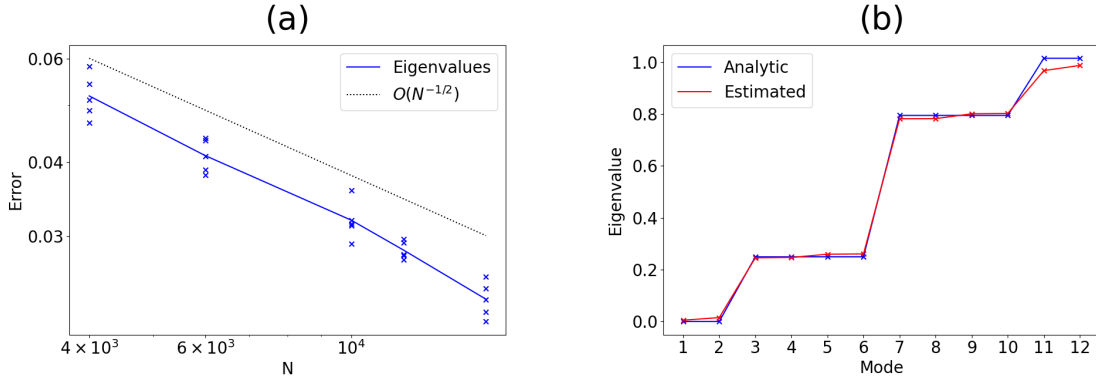


Figure 4: Operator estimation on torus with uniform sampling (with rejection) distribution. (a) Average of relative error (over the first 10 nontrivial) eigenvalues of the Hodge Laplacian estimator obtained from CMM as a function of N . (b) Mode by mode estimation for of spectrum for a single trial with $N = 16000$.

In this section, we demonstrate numerical convergence of CMM on the 2D torus. In particular, consider $M = \left\{ (2 + \cos\theta) \cos\phi, (2 + \cos\theta) \sin\phi, \sin\theta) : 0 \leq \theta, \phi \leq 2\pi \right\}$. To sample uniformly from the torus, we impose a rejection sampling scheme. Namely, we sample a pair $(\theta_i, \phi_i) \sim \text{Unif}([0, 2\pi]^2)$, along with a rejection parameter $w_i \sim \text{Unif}([0, 1])$. We accept the pair (θ_i, ϕ_i) if $w_i \leq (2/3 + \cos\theta_i/3)$, in which case we obtain a point $x_i = ((2 + \cos\theta_i) \cos\phi_i, (2 + \cos\theta_i) \sin\phi_i, \sin\theta_i)$. Otherwise, we reject. A dataset of size $N =$ generated in this way is shown in Figure 1b.

We remark that, on the torus, analytic eigen-solutions to the eigenvalue problem are not available for the Bochner and Hodge Laplacians. However, we can leverage the following result, along with semi-analytic eigen-solutions for the Laplace-Beltrami operator, to obtain semi-analytic eigenvalues for the Hodge Laplacian.

Theorem 5.1. *Let M denote a 2-dimensional manifold embedded in \mathbb{R}^3 . Then the nontrivial eigenvalues of the Hodge Laplacian are identical to the nontrivial eigenvalues of the Laplace-Beltrami operator where the multiplicities of eigenvalues of the Hodge Laplacian doubles those of the Laplace-Beltrami operator.*

The above is a standard result. A detailed proof can be found in [16]. Hence, to evaluate eigenvalue error, we combine the above result with semi-analytic eigen-solutions to the Laplace-Beltrami eigenvalue problem on the torus (following [16]). In particular, the Laplace-Beltrami eigenvalue problem on the 2D torus can be written in intrinsic coordinates as,

$$\Delta_M f_\ell = -\frac{1}{(2 + \cos\theta)^2} \frac{\partial^2 f_\ell}{\partial \phi^2} - \frac{\partial^2 f_\ell}{\partial \theta^2} + \frac{\sin\theta}{2 + \cos\theta} \frac{\partial f_\ell}{\partial \theta} = \lambda_\ell f_\ell.$$

Using separation of variables (assuming that $f_\ell(\theta, \phi) = \Phi_\ell(\phi)\Theta_\ell(\theta)$), we reduce the above to the following problems:

$$\Phi_\ell'' = m_\ell \Phi_\ell, \quad \Theta_\ell'' - \frac{\sin\theta}{2 + \cos\theta} \Theta_\ell' - \frac{m_\ell^2}{(2 + \cos\theta)^2} \Theta_\ell = \lambda_\ell \Theta_\ell.$$

The first can be solved analytically, while the second is solved numerically using a standard finite difference scheme on a fine grid. The resulting values for λ_ℓ are used to evaluate the error in Figure 4a. Here, we demonstrate the relative error in the estimation of the eigenvalues of the Hodge Laplacian estimated using CMM which numerically verifies the convergence reported in Corollary 4.1. Figure 4b shows the semi-analytic and estimated spectrum mode-by-mode for a single trial with $N = 16000$. CMM produces an accurate estimation, especially for modes 0-9.

5.3 Robustness to Noise

To investigate the effect of noise, we turn again to the unit sphere example. Consider the dataset of points N given by $x_i = (1 + \epsilon_i)\tilde{x}_i$ where $\tilde{x}_i \sim \text{Unif}(M)$, and $\epsilon_i \sim \text{Unif}([-\eta/2, \eta/2])$. Here, $\text{Unif}(M)$ denotes uniform sampling with respect to the volume measure of the manifold. To generate such samples, we follow the approach of Section 5.1. Numerical results for the computation of eigenvalues and eigenvectors for various values of η is shown in Figure 5.

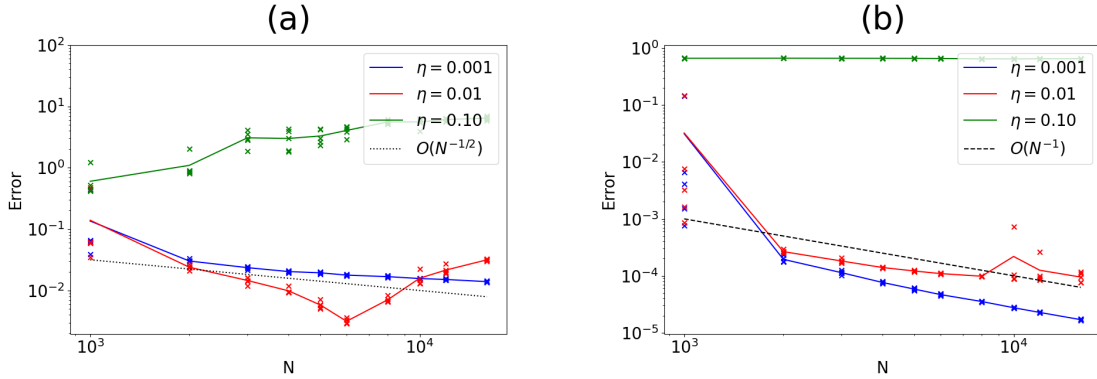


Figure 5: Operator estimation on a noisy sphere with uniform sampling distribution as functions of N . (a) Mean of percent error of eigenvalues. (b) Mean of mean-square-error of eigenvectors. Metrics are as defined in Equations (29) and (30). Color indicates noise level.

We see that when the noise is sufficiently small (0.1% of the radius of the sphere), convergence for both eigenvalues and eigenvectors is still obtained. When the noise is increased to 1.0%, while convergence still occurs for the eigenvector fields (red, Figure 5b), eigenvalue convergence for large N does not occur, though the error in this case is still relatively small. When the noise is increased to 10.0%, the results for both the eigenvalues and eigenvectors are inaccurate, and do not converge. Based on these results as well as the theoretical analysis, we suspect that the algorithm is robust to noise so long as the size of the noise ($\|x_i - \tilde{x}_i\|$ in this example) does not exceed the Monte-Carlo rate $O(N^{-1/2})$, which comes from integral estimation.

Given this analysis, there are many interesting future directions for modifying CMM to be more robust to noise. For instance, CMM hinges on the accurate estimation of tangent spaces (Section 2.1), which is in general sensitive to noise. One could employ more robust methods for approximating the tangent space on potentially noisy data (see, for instance, [9, 33]) and investigate how this affects the spectral error.

6 Summary

In this paper, we developed a numerical framework for approximating arbitrary differential operators in the weak form on Riemannian manifolds identified only by randomly sampled point cloud data. We proved, for the case

of estimating the Bochner Laplacian, the convergence of eigenvalues in high probability as $N \rightarrow \infty$, and provided several numerical examples validating this convergence in practice. This framework employs curved (nonlinear) local meshes, which are constructed by projecting point cloud data to the estimated tangent spaces [18] and the moving least squares parameterization [21], thus, allowing the curvature information such as Christoffel symbols to be appropriately accounted in the operator estimation. This approach is convenient as it avoids the curse of high ambient dimension, the construction of global parameterizations and meshes, and the tuning of various hyperparameters. Moreover, this method is flexible and is not restrictive to estimating only Laplacians. Theoretical and observed convergence rates, which for uniformly sampled data coincide with $O(N^{-1/d})$ for $d \geq 2$, are competitive with other estimators in the literature in the context of eigenvalue estimation for operators acting on vector fields on unknown manifolds. For instance, the spectral convergence of the RBF approximation to Bochner Laplacian was reported in [16] with convergence rate $O(N^{-1/d})$. As for the Graph Laplacian type method, the spectral convergence for the vector diffusion maps to the Bochner (or connection) Laplacian was established with no convergence rate as reported in [30]. Instead, they reported the pointwise convergence to the Bochner Laplacian acting on vector fields with convergence rate $O(N^{-\frac{1}{d/2+4}})$.

The ideas proposed in this paper suggest many potential directions for future work. Firstly, while the theoretical convergence results contain rates, these rates are not necessarily sharp. To this end, it is of interest to obtain lower bound estimates for the weak convergence result of Lemma 4.1. Secondly, this paper assumes that the underlying manifold is without boundary. Due to the weak formulation as well as the flexibility to apply the parameterizations from [21] to manifolds with boundary, it is natural to think that this method extends to the boundary without much modification. Nevertheless, details regarding local parameterization error analysis for points near the boundary remain to be seen. Third, throughout this manuscript, we consider polynomials of degree 2 since this is sufficient for the estimation of Christoffel symbols. However, theoretical analysis suggests that the rate of convergence for estimating the local charts can be increased by using higher-order approximations. A detailed theoretical and numerical analysis studying the benefits and drawbacks of employing this method with higher order polynomials, or different hypothesis spaces altogether, for the approximation of local parameterizations is of interest. Lastly, as we have shown in the last section, more work needs to be done to overcome noisy data.

Acknowledgment

The research of J.H. was partially supported by the NSF grants DMS-2207328, DMS-2229535, and the ONR grant N00014-22-1-2193.

A Example Computations for Local Curved Mesh Method

Throughout this appendix, local computations are done in terms of the metric computed in Section 2.4. For simplicity, we refer to the coordinates of this metric, the entries of this metric, the entries of its inverse, and Christoffel symbols in this metric as $\{\partial_{u_1}, \partial_{u_2}\}$, g_{ij} , g^{ij} , and Γ_{jk}^i , respectively. Explicit formulas for all quantities above can be deduced for the metric (12). For simplicity, we present the computations for $d = 2$.

The following notation will be necessary throughout. Fix a block i . Let $\mathbf{T} = [\mathbf{t}_1^{(i)}, \mathbf{t}_2^{(i)}, \dots, \mathbf{t}_n^{(i)}]$, the matrix whose columns form an orthonormal basis for the tangent space (first d components) and normal directions (last $n - d$ components) at i . Similarly, fix an arbitrary triangle $T_{i,r} \in R(i)$, and let $\mathbf{R}_{i,r} = [\partial_{u_1}, \partial_{u_2}]$ denote the matrix whose columns form a tangent space for the local curved mesh of triangle $T_{i,r}$, as defined in (11). We remark that $\mathbf{R}_{i,r}$ depends on the point (u_1, u_2) . Define

$$\mathbf{a}_k^{ij} = \mathbf{R}_{i,r}^{LS} \mathbf{T}^\top \mathbf{t}_k^{(j)}, \quad (31)$$

the vector of length d corresponding to the representation of $\mathbf{t}_k^{(j)}$ in the local coordinates, where the dependence of \mathbf{a}_k^{ij} on $T_{i,r}$ is understood. We note that $\mathbf{R}_{i,r}^{LS}$ is the least-squares solution for a map that takes the tangent vector $\mathbf{t}_k^{(j)}$ in the coordinates induced by columns of \mathbf{T} to the canonical \mathbb{R}^2 coordinates, which we denoted as \mathbf{a}_k^{ij} . With this representation, its clear that

$$\langle \mathbf{t}_{k_1}^{(i)}, \mathbf{t}_{k_2}^{(j)} \rangle_g = \langle g \mathbf{a}_{k_1}^{ii}, \mathbf{a}_{k_2}^{ij} \rangle = \left(\mathbf{a}_{k_1}^{ii} \right)^\top g \left(\mathbf{a}_{k_2}^{ij} \right), \quad (32)$$

as noted in (18) in Remark 3, where $g = g\Phi_{c_{i,r}}$ corresponds to the 2×2 metric tensor defined in (12).

In practice, since a smooth vector field $W : M \rightarrow TM$ can be represented locally on a neighborhood of $T_{x_i}M$, and for sufficiently large N (such that the curvature between neighboring points of data is sufficiently small), $R(i)$ is contained in this neighborhood, instead of \mathbf{T} , one can use $\mathbf{T}_i = [\mathbf{t}_1^{(i)}, \dots, \mathbf{t}_d^{(i)}]$, and subsequently ignore the last $(n-d)$ columns of $\mathbf{R}_{i,r}$, which reduces computation time as the first d rows of $\mathbf{R}_{i,r}$ do not depend on the point (u_1, u_2) ; see (11). We observe the difference in estimated eigenvalues and eigenvector fields when using the full matrices as in (31) and the reduced approach outlined above is negligible.

We remark that computations corresponding to off-diagonal matrix elements simplify significantly. In particular, integrals corresponding to the (i, j) -th entry for $i \neq j$ vanish for each $T_{i,r} \in R(i)$ except those for which the edge connecting $\vec{0}$ and $\mathbf{T}_i^\top(x_j - x_i)$, is a side of $T_{i,r}$. Since $T_{i,r}$ is a triangle with vertices $\{\vec{0}, \vec{v}_{i_{j_r}}, \vec{v}_{i_{k_r}}\}$, this is simply stating that $\mathbf{T}_i^\top(x_j - x_i)$ is a node of $T_{i,r}$. Therefore, for future convenience, we denote

$$Q(i, j) = \{T_{i,r} \in R(i) : \mathbf{T}_i^\top(x_j - x_i) \text{ is a node of } T_{i,r}\}.$$

A.1 Mass matrix for operators on vector fields

Here we explicitly compute the mass matrix for vector-fields, \mathbf{M} . The diagonal block formula from before reads

$$\begin{bmatrix} [\mathbf{M}]_{2i-1,2j-1} & [\mathbf{M}]_{2i-1,2j} \\ [\mathbf{M}]_{2i,2j-1} & [\mathbf{M}]_{2i,2j} \end{bmatrix} = \sum_{T_{i,r} \in R(i)} \int_T e_i e_j \begin{bmatrix} \langle \mathbf{t}_1^{(i)}, \mathbf{t}_1^{(j)} \rangle_g & \langle \mathbf{t}_1^{(i)}, \mathbf{t}_2^{(j)} \rangle_g \\ \langle \mathbf{t}_2^{(i)}, \mathbf{t}_1^{(j)} \rangle_g & \langle \mathbf{t}_2^{(i)}, \mathbf{t}_2^{(j)} \rangle_g \end{bmatrix} \sqrt{\det(g)} du_1 du_2,$$

Since we compute each integral with a quadrature rule on the vertices, it suffices to compute the integrand at an arbitrary point (u_1, u_2) .

To begin, we compute the diagonal block components. When $i = j$, we have

$$\begin{bmatrix} [\mathbf{M}]_{2i-1,2i-1} & [\mathbf{M}]_{2i-1,2i} \\ [\mathbf{M}]_{2i,2i-1} & [\mathbf{M}]_{2i,2i} \end{bmatrix} = \sum_{T_{i,r} \in R(i)} \int_T (1 - u_1 - u_2)^2 \begin{bmatrix} \langle \mathbf{g}\mathbf{a}_1^{ii}, \mathbf{a}_1^{ii} \rangle & \langle \mathbf{g}\mathbf{a}_1^{ii}, \mathbf{a}_2^{ii} \rangle \\ \langle \mathbf{g}\mathbf{a}_2^{ii}, \mathbf{a}_1^{ii} \rangle & \langle \mathbf{g}\mathbf{a}_2^{ii}, \mathbf{a}_2^{ii} \rangle \end{bmatrix} \sqrt{\det(g)} du_1 du_2,$$

where we have used (32). We remark that the quantities above indeed depend on each triangle $T_{i,r}$.

When $j \neq i$, we recall that the only two triangles for which the integration is nonzero are those in $Q(i, j)$ (which consists of 0 or 2 triangles). In both of these triangles, we can reorder the vertices so that $(1, 0) \rightarrow \mathbf{T}_i^\top(x_j - x_i)$. Hence, a nonzero of diagonal block of the mass matrix takes the form

$$\begin{bmatrix} [\mathbf{M}]_{2i-1,2j-1} & [\mathbf{M}]_{2i-1,2j} \\ [\mathbf{M}]_{2i,2j-1} & [\mathbf{M}]_{2i,2j} \end{bmatrix} = \sum_{T_{i,r} \in Q(i,j)} \int_T (1 - u_1 - u_2) u_1 \begin{bmatrix} \langle \mathbf{g}\mathbf{a}_1^{ii}, \mathbf{a}_1^{ij} \rangle & \langle \mathbf{g}\mathbf{a}_1^{ii}, \mathbf{a}_2^{ij} \rangle \\ \langle \mathbf{g}\mathbf{a}_2^{ii}, \mathbf{a}_1^{ij} \rangle & \langle \mathbf{g}\mathbf{a}_2^{ii}, \mathbf{a}_2^{ij} \rangle \end{bmatrix} \sqrt{\det(g)} du_1 du_2.$$

A.2 Stiffness Matrix for Bochner Laplacian

The Bochner Laplacian $\Delta_B : TM \rightarrow TM$ can be (weakly) defined by the following formula:

$$\langle \Delta_B w, v \rangle_g = \langle \text{grad}_g w, \text{grad}_g v \rangle_g \quad (33)$$

where the gradient grad_g of a vector field $v = v^i \frac{\partial}{\partial u^i}$ is a $(2, 0)$ tensor field given by

$$\text{grad}_g v = g^{kj} \left(\frac{\partial v^i}{\partial u^k} + v^p \Gamma_{pk}^i \right) \frac{\partial}{\partial u^i} \otimes \frac{\partial}{\partial u^j}.$$

Notice that (33) denotes the Riemmanian inner product of two $(2, 0)$ tensor fields. Recall that for tensor fields $a = a_{ij} \frac{\partial}{\partial u_1} \otimes \frac{\partial}{\partial u_2}$ and $b = b_{ij} \frac{\partial}{\partial u_1} \otimes \frac{\partial}{\partial u_2}$, the Riemannian inner product is defined as,

$$\langle a, b \rangle_g = \sum_{i,j,k,\ell} a_{ij} g_{ik} b_{k\ell} g_{j\ell}.$$

Interpreting a, b , and g as matrices written in the basis $\{\frac{\partial}{\partial u_i} \otimes \frac{\partial}{\partial u_j}\}_{i,j=1}^d$, it is not difficult to show that this can be rewritten

$$\langle a, b \rangle_g = \text{trace}(agb^\top g).$$

In this section, we compute the integrands necessary for employing the local mesh method with $D = \text{grad}_g$. Recall the blockwise formula for the stiffness matrix:

$$\begin{bmatrix} [\mathbf{S}]_{2i-1,2j-1} & [\mathbf{S}]_{2i-1,2j} \\ [\mathbf{S}]_{2i,2j-1} & [\mathbf{S}]_{2i,2j} \end{bmatrix} = \sum_{T_{i,r} \in R(i)} \int_T \begin{bmatrix} \langle \text{grad}_g e_i \mathbf{t}_1^{(i)}, \text{grad}_g e_j \mathbf{t}_1^{(j)} \rangle_g & \langle \text{grad}_g e_i \mathbf{t}_1^{(i)}, \text{grad}_g e_j \mathbf{t}_2^{(j)} \rangle_g \\ \langle \text{grad}_g e_i \mathbf{t}_2^{(i)}, \text{grad}_g e_j \mathbf{t}_1^{(j)} \rangle_g & \langle \text{grad}_g e_i \mathbf{t}_2^{(i)}, \text{grad}_g e_j \mathbf{t}_2^{(j)} \rangle_g \end{bmatrix} \sqrt{\det(g)} du_1 du_2.$$

We begin by computing the diagonal case, $\langle \text{grad}_g e_i \mathbf{t}_{k_1}^{(i)}, \text{grad}_g e_i \mathbf{t}_{k_2}^{(i)} \rangle_g$.

Simplifying the abuse of notation, we have

$$\langle \text{grad}_g e_i \mathbf{t}_{k_1}^{(i)}, \text{grad}_g e_i \mathbf{t}_{k_2}^{(j)} \rangle_g = \text{trace} \left(\mathbf{A}_{k_1}^{ii} g (\mathbf{A}_{k_2}^{ii})^\top g \right). \quad (34)$$

where $\mathbf{A}_{k_1}^{ii}, \mathbf{A}_{k_2}^{ii}$ correspond to the 2×2 matrix representations of $(2, 0)$ tensor fields

$$\begin{aligned} \mathbf{A}_{k_1}^{ii} &= \text{grad}_g \left[(1 - u_1 - u_2) (\mathbf{a}_{k_1}^{ii})_1 \partial_{u_1} + (1 - u_1 - u_2) (\mathbf{a}_{k_1}^{ii})_2 \partial_{u_2} \right], \\ \mathbf{A}_{k_2}^{ii} &= \text{grad}_g \left[(1 - u_1 - u_2) (\mathbf{a}_{k_2}^{ii})_1 \partial_{u_1} + (1 - u_1 - u_2) (\mathbf{a}_{k_2}^{ii})_2 \partial_{u_2} \right] \end{aligned}$$

in the basis of $\{\partial_{u_i} \otimes \partial_{u_j}\}_{i,j}$. By linearity, we have

$$\begin{aligned} \mathbf{A}_{k_1}^{ii} &= (\mathbf{a}_{k_1}^{(ii)})_1 \text{grad}_g [(1 - u_1 - u_2) \partial_{u_1}] + (\mathbf{a}_{k_1}^{(ii)})_2 \text{grad}_g [(1 - u_1 - u_2) \partial_{u_2}] \\ \mathbf{A}_{k_2}^{ii} &= (\mathbf{a}_{k_2}^{(ii)})_1 \text{grad}_g [(1 - u_1 - u_2) \partial_{u_1}] + (\mathbf{a}_{k_2}^{(ii)})_2 \text{grad}_g [(1 - u_1 - u_2) \partial_{u_2}]. \end{aligned}$$

It remains to compute the matrices $\text{grad}_g [(1 - u_1 - u_2) \partial_{u_1}]$, $\text{grad}_g [(1 - u_1 - u_2) \partial_{u_2}]$, which amounts to plugging in to the local formula for grad_g . In our case, gradient of a vector field $v = v^i \frac{\partial}{\partial u_i}$, where $v^1 = 1 - u_1 - u_2$ and $v^2 = 0$, is given as,

$$\text{grad}_g v = g^{kj} \left(\frac{\partial v^i}{\partial u_k} + v^p \Gamma_{pk}^i \right) \partial_{u_i} \otimes \partial_{u_j}.$$

Expanding each component, we have

$$\begin{aligned} \text{grad}_g [(1 - u_1 - u_2) \partial_{u_1}] &= g^{k1} \left(\frac{\partial(1 - u_1 - u_2)}{\partial u_k} + (1 - u_1 - u_2) \Gamma_{1k}^1 \right) \partial_{u_1} \otimes \partial_{u_1} \\ &\quad + g^{k2} \left(\frac{\partial(1 - u_1 - u_2)}{\partial u_k} + (1 - u_1 - u_2) \Gamma_{1k}^1 \right) \partial_{u_1} \otimes \partial_{u_2} \\ &\quad + g^{k1} ((1 - u_1 - u_2) \Gamma_{1k}^2) \partial_{u_2} \otimes \partial_{u_1} + g^{k2} ((1 - u_1 - u_2) \Gamma_{1k}^2) \partial_{u_2} \otimes \partial_{u_2} \\ &= (-g^{11} - g^{21} + (1 - u_1 - u_2) (\Gamma_{11}^1 g^{11} + \Gamma_{12}^1 g^{21})) \partial_{u_1} \otimes \partial_{u_1} \\ &\quad + (-g^{12} - g^{22} + (1 - u_1 - u_2) (\Gamma_{11}^1 g^{12} + \Gamma_{12}^1 g^{22})) \partial_{u_1} \otimes \partial_{u_2} \\ &\quad + ((1 - u_1 - u_2) (\Gamma_{11}^2 g^{11} + \Gamma_{12}^2 g^{21})) \partial_{u_2} \otimes \partial_{u_1} \\ &\quad + ((1 - u_1 - u_2) (\Gamma_{11}^2 g^{12} + \Gamma_{12}^2 g^{22})) \partial_{u_2} \otimes \partial_{u_2} \end{aligned}$$

which can be written in matrix form as follows:

$$\text{grad}_g [(1 - u_1 - u_2) \partial_{u_1}] = \left((1 - u_1 - u_2) \begin{bmatrix} \Gamma_{11}^1 & \Gamma_{12}^1 \\ \Gamma_{11}^2 & \Gamma_{12}^2 \end{bmatrix} + \begin{bmatrix} -1 & -1 \\ 0 & 0 \end{bmatrix} \right) g^{-1}$$

Following the same calculation, we have:

$$\text{grad}_g [(1 - u_1 - u_2) \partial_{u_2}] = \left((1 - u_1 - u_2) \begin{bmatrix} \Gamma_{21}^1 & \Gamma_{22}^1 \\ \Gamma_{21}^2 & \Gamma_{22}^2 \end{bmatrix} + \begin{bmatrix} 0 & 0 \\ -1 & -1 \end{bmatrix} \right) g^{-1}.$$

This completes the computation for $i = j$. When $i \neq j$, we instead have

$$\langle \text{grad}_g e_i \mathbf{t}_{k_1}^{(i)}, \text{grad}_g e_i \mathbf{t}_{k_2}^{(j)} \rangle_g = \text{trace} \left(\mathbf{A}_{k_1}^{ii} g (\mathbf{A}_{k_2}^{ij})^\top g \right),$$

where

$$\mathbf{A}_{k_2}^{ij} = (\mathbf{a}_{k_2}^{ij})_1 \text{grad}_g [u_1 \partial_{u_1}] + (\mathbf{a}_{k_2}^{ij})_2 \text{grad}_g [u_1 \partial_{u_2}].$$

where u_1 in the above is obtained by reordering the vertices of a single triangle. The final quantities to compute are given by

$$\begin{aligned} \text{grad}_g [u_1 \partial_{u_1}] &= \left(u_1 \begin{bmatrix} \Gamma_{11}^1 & \Gamma_{12}^1 \\ \Gamma_{11}^2 & \Gamma_{12}^2 \end{bmatrix} + \begin{bmatrix} 1 & 0 \\ 0 & 0 \end{bmatrix} \right) g^{-1} \\ \text{grad}_g [u_1 \partial_{u_2}] &= \left(u_1 \begin{bmatrix} \Gamma_{21}^1 & \Gamma_{22}^1 \\ \Gamma_{21}^2 & \Gamma_{22}^2 \end{bmatrix} + \begin{bmatrix} 0 & 0 \\ 1 & 0 \end{bmatrix} \right) g^{-1}. \end{aligned}$$

In summary, when $i = j$,

$$\begin{bmatrix} [\mathbf{S}]_{2i-1,2i-1} & [\mathbf{S}]_{2i-1,2i} \\ [\mathbf{S}]_{2i,2i-1} & [\mathbf{S}]_{2i,2i} \end{bmatrix} = \sum_{T_{i,r} \in R(i)} \int_T \begin{bmatrix} \text{trace}(\mathbf{A}_1^{ii} g(\mathbf{A}_1^{ii})^\top g) & \text{trace}(\mathbf{A}_1^{ii} g(\mathbf{A}_2^{ii})^\top g) \\ \text{trace}(\mathbf{A}_2^{ii} g(\mathbf{A}_1^{ii})^\top g) & \text{trace}(\mathbf{A}_2^{ii} g(\mathbf{A}_2^{ii})^\top g) \end{bmatrix} \sqrt{\det(g)} du_1 du_2,$$

while for $i \neq j$, we have

$$\begin{bmatrix} [\mathbf{S}]_{2i-1,2j-1} & [\mathbf{S}]_{2i-1,2j} \\ [\mathbf{S}]_{2i,2j-1} & [\mathbf{S}]_{2i,2j} \end{bmatrix} = \sum_{T_{i,r} \in Q(i,j)} \int_T \begin{bmatrix} \text{trace}(\mathbf{A}_1^{ii} g(\mathbf{A}_1^{jj})^\top g) & \text{trace}(\mathbf{A}_1^{ii} g(\mathbf{A}_2^{jj})^\top g) \\ \text{trace}(\mathbf{A}_2^{ii} g(\mathbf{A}_1^{jj})^\top g) & \text{trace}(\mathbf{A}_2^{ii} g(\mathbf{A}_2^{jj})^\top g) \end{bmatrix} \sqrt{\det(g)} du_1 du_2,$$

where in each case, A_k^{ij} are as defined above.

A.3 Stiffness Matrix for Hodge Laplacian

The Hodge Laplacian is typically defined on a k -form ω by the formula

$$\Delta_H \omega = d^* d \omega + d d^* \omega$$

where d denotes the total differential, and d^* is the codifferential. The Hodge Laplacian can also be defined on vector fields by leveraging the musical isomorphisms:

$$\Delta_H v := \sharp(d^* d \omega + d d^* \omega) \flat v,$$

For the purposes of this paper, only the weak form is necessary:

$$\langle \Delta_H v, w \rangle_g = \langle d \flat v, d \flat w \rangle_g + \langle d^* \flat v, d^* \flat w \rangle_g, \quad (35)$$

for any $v, w \in \mathfrak{X}(M)$, so the first inner-product is defined over 2-forms (or $(0,2)$ -tensors) whereas the second inner product is defined over 0-forms (or functions). Based on the above formula, all that is needed for computations is the action of d and d^* on 1-forms (on manifolds of dimension 2). These formulas are given by

$$\begin{aligned} d(\omega_i du^i) &= \frac{\partial \omega_i}{\partial u^j} du^j, \\ d^*(\omega_i du^i) &= (-1) \star d \star (\omega_i du^i), \end{aligned}$$

where \star denotes the hodge star operator, which is defined locally on a k -form ω to be the unique $(d-k)$ form $\star \omega$ satisfying the formula

$$\omega' \wedge \star \omega = \langle \omega', \omega \rangle_g \sqrt{\det g} du_1 \wedge du_2$$

for any k -form ω' . Since (35), as well as the above formula, contains inner-products of k -forms, we remind the reader that the inner product of two k forms is given by

$$\langle \omega^1 \wedge \dots \wedge \omega^k, \eta^1 \wedge \dots \wedge \eta^k \rangle = \det(\langle \omega^i, \eta^j \rangle_g).$$

The definition for the stiffness matrix can be initially simplified as follows:

$$\begin{bmatrix} [\mathbf{S}]_{2i-1,2j-1} & [\mathbf{S}]_{2i-1,2j} \\ [\mathbf{S}]_{2i,2j-1} & [\mathbf{S}]_{2i,2j} \end{bmatrix} = \sum_{T_{i,r} \in R(i)} \int_T \begin{bmatrix} \langle d \flat e_i \mathbf{t}_1^{(i)}, d \flat e_j \mathbf{t}_1^{(j)} \rangle_g + \langle d^* \flat e_i \mathbf{t}_1^{(i)}, d^* \flat e_j \mathbf{t}_1^{(j)} \rangle_g & \langle d \flat e_i \mathbf{t}_1^{(i)}, d \flat e_j \mathbf{t}_2^{(j)} \rangle_g + \langle d^* \flat e_i \mathbf{t}_1^{(i)}, d^* \flat e_j \mathbf{t}_2^{(j)} \rangle_g \\ \langle d \flat e_i \mathbf{t}_2^{(i)}, d \flat e_j \mathbf{t}_1^{(j)} \rangle_g + \langle d^* \flat e_i \mathbf{t}_2^{(i)}, d^* \flat e_j \mathbf{t}_1^{(j)} \rangle_g & \langle d \flat e_i \mathbf{t}_2^{(i)}, d \flat e_j \mathbf{t}_2^{(j)} \rangle_g + \langle d^* \flat e_i \mathbf{t}_2^{(i)}, d^* \flat e_j \mathbf{t}_2^{(j)} \rangle_g \end{bmatrix} \sqrt{\det(g)} du_1 du_2. \quad (36)$$

We'll begin by computing $d \flat v$ and $d^* \flat v$ on basis functions in each case. Note that in general, the nodal basis functions are a linear combination of

$$v = c_1 \hat{\phi} \frac{\partial}{\partial u_1} + c_2 \hat{\phi} \frac{\partial}{\partial u_2},$$

where $\hat{\phi} = 1 - u_1 - u_2$, or

$$v = c_1 u_1 \frac{\partial}{\partial u_1} + c_2 u_1 \frac{\partial}{\partial u_2}.$$

Hence, we handle the following four cases:

$$\begin{aligned}
\text{case 1:} \quad & v - (1 - u_1 - u_2) \frac{\partial}{\partial u_1} \\
\text{case 2:} \quad & v = (1 - u_1 - u_2) \frac{\partial}{\partial u_2} \\
\text{case 3:} \quad & v = u_1 \frac{\partial}{\partial u_1} \\
\text{case 4:} \quad & v = u_1 \frac{\partial}{\partial u_2}
\end{aligned}$$

For case 1, we have $\flat v = (1 - u_1 - u_2)g_{11}du_1 + (1 - u_1 - u_2)g_{12}du_2$. Hence,

$$\begin{aligned}
dbv &= \frac{\partial(g_{11}\hat{\phi})}{\partial u_2} du_2 \wedge du_1 + \frac{\partial(g_{12}\hat{\phi})}{\partial u_1} du_1 \wedge du_2 = \left(\frac{\partial(g_{12}\hat{\phi})}{\partial u_1} - \frac{\partial(g_{11}\hat{\phi})}{\partial u_2} \right) du_1 \wedge du_2 \\
&= \left(g_{11} - g_{12} + \hat{\phi} \frac{\partial g_{12}}{\partial u_1} - \hat{\phi} \frac{\partial g_{11}}{\partial u_2} \right) du_1 \wedge du_2 := A_1 du_1 \wedge du_2.
\end{aligned}$$

Similarly, we have that

$$d^* \flat v = (-1) \star d \star (\hat{\phi} g_{11} du_1 + \hat{\phi} g_{12} du_2).$$

The formula for \star shows that $\star(du_1) = -g^{12}\sqrt{\det(g)}du_1 + g^{11}\sqrt{\det(g)}du_2$, $\star(du_2) = -g^{22}\sqrt{\det(g)}du_1 + g^{12}\sqrt{\det(g)}du_2$, and $\star(du_1 \wedge du_2) = \det(g^{-1})\sqrt{\det(g)} = (\det(g))^{-1/2}$. Hence,

$$\begin{aligned}
d^* \flat v &= (-1) \star d \left(\hat{\phi} \sqrt{\det(g)} \left((-g_{11}g^{12} - g_{12}g^{22}) du_1 + (g_{12}g^{12} + g_{11}g^{11}) du_2 \right) \right) \\
&= (-1) \star d \left(\hat{\phi} \sqrt{\det(g)} (1 du_2) \right) \\
&= (-1) \star \left(\frac{\partial}{\partial u_1} \left(\hat{\phi} \sqrt{\det(g)} \right) du_1 \wedge du_2 \right) \\
&= \frac{-1}{\sqrt{\det(g)}} \left(\frac{\partial}{\partial u_1} \left(\hat{\phi} \sqrt{\det(g)} \right) \right) \\
&= 1 - \frac{\hat{\phi}}{\sqrt{\det g}} \frac{\partial \sqrt{\det g}}{\partial u_1} := A_3
\end{aligned}$$

Similar computations yield the results for other three cases. The results are as follows:

$$\begin{aligned}
\text{case 2:} \quad & dbv = \left(g_{12} - g_{22} + \hat{\phi} \frac{\partial g_{22}}{\partial u_1} - \hat{\phi} \frac{\partial g_{12}}{\partial u_2} \right) du_1 \wedge du_2 := A_2 du_1 \wedge du_2 \\
& d^* \flat v = 1 - \frac{\hat{\phi}}{\sqrt{\det g}} \frac{\partial \sqrt{\det g}}{\partial u_2} := A_4 \\
\text{case 3:} \quad & dbv = \left(g_{21} + u_1 \frac{\partial g_{21}}{\partial u_1} - u_1 \frac{\partial g_{11}}{\partial u_2} \right) du_1 \wedge du_2 := B_1 du_1 \wedge du_2 \\
& d^* \flat v = -1 - \frac{u_1}{\sqrt{\det g}} \frac{\partial \sqrt{\det g}}{\partial u_1} := B_3 \\
\text{case 4:} \quad & dbv = \left(g_{22} + u_1 \frac{\partial g_{22}}{\partial u_1} - u_1 \frac{\partial g_{12}}{\partial u_2} \right) du_1 \wedge du_2 := B_2 du_1 \wedge du_2 \\
& d^* \flat v = -\frac{u_1}{\sqrt{\det g}} \frac{\partial \sqrt{\det g}}{\partial u_2} := B_4.
\end{aligned}$$

We can now compute the first term completely in the two cases: the diagonal blocks, and the off diagonal blocks. On the diagonal blocks, (meaning $i = j$), we have

$$\begin{aligned}
\langle dbe_i \mathbf{t}_r^{(i)}, dbe_i \mathbf{t}_s^{(i)} \rangle_g &= (\mathbf{a}_r^{ii})_1 (\mathbf{a}_s^{ii})_1 A_1^2 \langle du_1 \wedge du_2, du_1 \wedge du_2 \rangle_g + (\mathbf{a}_r^{ii})_2 (\mathbf{a}_s^{ii})_1 A_1 A_2 \langle du_1 \wedge du_2, du_1 \wedge du_2 \rangle_g \\
&+ (\mathbf{a}_r^{ii})_1 (\mathbf{a}_s^{ii})_2 A_1 A_2 \langle du_1 \wedge du_2, du_1 \wedge du_2 \rangle_g + (\mathbf{a}_r^{ii})_2 (\mathbf{a}_s^{ii})_2 A_2^2 \langle du_1 \wedge du_2, du_1 \wedge du_2 \rangle_g \\
&= \frac{1}{\det g} \left((\mathbf{a}_r^{ii})_1 (\mathbf{a}_s^{ii})_1 A_1^2 + (\mathbf{a}_r^{ii})_2 (\mathbf{a}_s^{ii})_1 A_1 A_2 + (\mathbf{a}_r^{ii})_1 (\mathbf{a}_s^{ii})_2 A_1 A_2 + (\mathbf{a}_r^{ii})_2 (\mathbf{a}_s^{ii})_2 A_2^2 \right) \quad (37)
\end{aligned}$$

Similarly,

$$\langle d^* \mathbf{b} e_i \mathbf{t}_r^{(i)}, d^* \mathbf{b} e_i \mathbf{t}_s^{(i)} \rangle_g = \left((\mathbf{a}_r^{ii})_1 (\mathbf{a}_s^{ii})_1 A_3^2 + (\mathbf{a}_r^{ii})_2 (\mathbf{a}_s^{ii})_1 A_3 A_4 + (\mathbf{a}_r^{ii})_1 (\mathbf{a}_s^{ii})_2 A_3 A_4 + (\mathbf{a}_r^{ii})_2 (\mathbf{a}_s^{ii})_2 A_4^2 \right). \quad (38)$$

Whence, its clear that the formula for the stiffness matrix on the diagonal elements is given by (36), plugging in the computed values from (37), (38).

On the off diagonal blocks, (meaning $i \neq j$), we have

$$\begin{aligned} \langle d \mathbf{b} e_i \mathbf{t}_r^{(i)}, d \mathbf{b} e_i \mathbf{t}_s^{(j)} \rangle_g &= (\mathbf{a}_r^{ii})_1 (\mathbf{a}_s^{ij})_1 A_1 B_1 \langle d u_1 \wedge d u_2, d u_1 \wedge d u_2 \rangle_g + (\mathbf{a}_r^{ii})_1 (\mathbf{a}_s^{ij})_2 A_1 B_2 \langle d u_1 \wedge d u_2, d u_1 \wedge d u_2 \rangle_g \\ &+ (\mathbf{a}_r^{ii})_2 (\mathbf{a}_s^{ij})_1 A_2 B_1 \langle d u_1 \wedge d u_2, d u_1 \wedge d u_2 \rangle_g + (\mathbf{a}_r^{ii})_2 (\mathbf{a}_s^{ij})_2 A_2 B_2 \langle d u_1 \wedge d u_2, d u_1 \wedge d u_2 \rangle_g \\ &= \frac{1}{\det g} \left((\mathbf{a}_r^{ii})_1 (\mathbf{a}_s^{ij})_1 A_1 B_1 + (\mathbf{a}_r^{ii})_1 (\mathbf{a}_s^{ij})_2 A_1 B_2 + (\mathbf{a}_r^{ii})_2 (\mathbf{a}_s^{ij})_1 A_2 B_1 + (\mathbf{a}_r^{ii})_2 (\mathbf{a}_s^{ij})_2 A_2 B_2 \right). \end{aligned} \quad (39)$$

Similarly,

$$\langle d^* \mathbf{b} e_i \mathbf{t}_r^{(i)}, d^* \mathbf{b} e_i \mathbf{t}_s^{(j)} \rangle_g = \left((\mathbf{a}_r^{ii})_1 (\mathbf{a}_s^{ij})_1 A_3 B_3 + (\mathbf{a}_r^{ii})_2 (\mathbf{a}_s^{ij})_1 B_3 A_4 + (\mathbf{a}_r^{ii})_1 (\mathbf{a}_s^{ij})_2 A_3 B_4 + (\mathbf{a}_r^{ii})_2 (\mathbf{a}_s^{ij})_2 A_4 B_4 \right). \quad (40)$$

From this, its clear that when $i = j$, the formula for thee stiffness matrix is given by (36), plugging in the computed values from (39), (40).

B Proofs of Technical Lemmas

Proof of Lemma 4.2. For simplicity of notation, we do not explicitly write evaluation of each quantity on \vec{v} . First, notice that

$$\begin{aligned} \partial_{v_1}(\gamma_{x_i}) &= \left(1, 0, \frac{\partial z_{x_i}}{\partial v_1} \right)^\top, \\ \partial_{v_2}(\gamma_{x_i}) &= \left(0, 1, \frac{\partial z_{x_i}}{\partial v_2} \right)^\top. \end{aligned}$$

Similarly,

$$\begin{aligned} \partial_{v_1}(\alpha_{x_i}) &= \left(1, 0, \frac{\partial p_i}{\partial v_1} \right)^\top \\ \partial_{v_2}(\alpha_{x_i}) &= \left(0, 1, \frac{\partial p_i}{\partial v_2} \right)^\top. \end{aligned}$$

Using (25), we see that

$$\| \partial_{v_k}(\gamma_{x_i})(\vec{v}) - \partial_{v_k}(\alpha_{x_i})(\vec{v}) \| = O(h_{X,M}^2).$$

Moreover, adding and subtracting $(\partial p_i / \partial v_q)(\partial z_{x_i} / \partial v_s)$, we find that

$$\begin{aligned} |(g_{\alpha_{x_i}})_{qs} - (g_{\gamma_{x_i}})_{qs}| &\leq |(\partial p_i / \partial v_q)(\partial p_i / \partial v_s) - (\partial p_i / \partial v_q)(\partial z_{x_i} / \partial v_s)| \\ &+ |(\partial p_i / \partial v_q)(\partial z_{x_i} / \partial v_s) - (\partial z_{x_i} / \partial v_q)(\partial z_{x_i} / \partial v_s)| \\ &= O(h_{X,M}^2). \end{aligned}$$

Similarly, adding and subtracting $(g_{\alpha_{x_i}})_{11}(g_{\gamma_{x_i}})_{22} + (g_{\alpha_{x_i}})_{12}(g_{\gamma_{x_i}})_{21}$, we have that

$$\begin{aligned} |\det(g_{\gamma_{x_i}}) - \det(g_{p_i})| &\leq \left| (g_{\gamma_{x_i}})_{11}(g_{\gamma_{x_i}})_{22} - (g_{\alpha_{x_i}})_{11}(g_{\gamma_{x_i}})_{22} \right| \\ &+ \left| (g_{\alpha_{x_i}})_{11}(g_{\gamma_{x_i}})_{22} - (g_{\alpha_{x_i}})_{11}(g_{\alpha_{x_i}})_{22} \right| \\ &+ \left| (g_{\gamma_{x_i}})_{12}(g_{\gamma_{x_i}})_{21} - (g_{\alpha_{x_i}})_{12}(g_{\gamma_{x_i}})_{21} \right| \\ &+ \left| (g_{\alpha_{x_i}})_{12}(g_{\gamma_{x_i}})_{21} - (g_{\alpha_{x_i}})_{12}(g_{\alpha_{x_i}})_{21} \right| \\ &= O(h_{X,M}^2). \end{aligned}$$

Since $\det(g_{\gamma_{x_i}})$ is bounded away from 0 independent of x_i , we have that

$$\left| \sqrt{\det(g_{\gamma_{x_i}})} - \sqrt{\det(g_{p_i})} \right| = O(h_{X,M}).$$

Using the above facts along with the entrywise formula for the coefficients of the inverse (see, for instance, Chapter 5, Theorem 7 of [19]), its immediate to see that,

$$\left| g_{\gamma_{x_i}}^{qs} - g_{p_i}^{qs} \right| = O(h_{X,M}).$$

For the Christoffel symbols, recall that p_i can estimate two derivatives of z_{x_i} up to order $h_{X,M}$. Since

$$\begin{aligned} \frac{\partial(g_{\gamma_{x_i}})_{qs}}{\partial v_t} &= (\partial^2 z_{x_i} / \partial v_q v_t)(\partial z_{x_i} / \partial v_s) + (\partial z_{x_i} / \partial v_q)(\partial^2 z_{x_i} / \partial v_s v_t) \\ \frac{\partial(g_{\alpha_{x_i}})_{qs}}{\partial v_t} &= (\partial^2 p_i / \partial v_q v_t)(\partial p_i / \partial v_s) + (\partial p_i / \partial v_q)(\partial^2 p_i / \partial v_s v_t), \end{aligned}$$

adding and subtracting $(\partial^2 z_{x_i} / \partial v_q v_t)(\partial p_i / \partial v_s) + (\partial z_{x_i} / \partial v_q)(\partial^2 p_i / \partial v_s v_t)$, we see that

$$\begin{aligned} \left| \partial(g_{\gamma_{x_i}})_{qs} / \partial v_t - \partial(g_{p_i})_{qs} / \partial v_t \right| &\leq \left| (\partial^2 z_{x_i} / \partial v_q v_t)(\partial z_{x_i} / \partial v_s) - (\partial^2 z_{x_i} / \partial v_q v_t)(\partial p_i / \partial v_s) \right| \\ &\quad + \left| (\partial^2 z_{x_i} / \partial v_q v_t)(\partial p_i / \partial v_s) - (\partial^2 p_i / \partial v_q v_t)(\partial p_i / \partial v_s) \right| \\ &\quad + \left| (\partial z_{x_i} / \partial v_q)(\partial^2 z_{x_i} / \partial v_s v_t) - (\partial z_{x_i} / \partial v_q)(\partial^2 p_i / \partial v_s v_t) \right| \\ &\quad + \left| (\partial z_{x_i} / \partial v_q)(\partial^2 p_i / \partial v_s v_t) - (\partial p_i / \partial v_q)(\partial^2 p_i / \partial v_s v_t) \right| \\ &= O(h_{X,M}). \end{aligned}$$

Plugging into the well known formula for the Christoffel symbols in terms of the metric tensor and leveraging estimates above, it follows immediately that

$$\left| \Gamma_{st}^q(p_i) - \Gamma_{st}^q(\gamma_{x_i}) \right| = O(h_{X,M}).$$

This completes the proof. \square

Proof of Lemma 4.4. It follows from Lemmas 4.2 and 4.3 that

$$\begin{aligned} |g_{\gamma_{x_i}}^{sj} - g_{\alpha_{x_i}}^{sj}| &= O(h_{X,M}), & |(g_{\gamma_{x_i}})_{sj} - (g_{\alpha_{x_i}})_{sj}| &= O(h_{X,M}) \\ |W^p - \widehat{W}^p| &= O(h_{X,M}), & \left| \frac{\partial W^t}{\partial v_s} - \frac{\partial \widehat{W}^t}{\partial v_s} \right| &= O(h_{X,M}) \\ |\Gamma_{ps}^t(\gamma_{x_i}) - \Gamma_{ps}^t(\alpha_{x_i})| &= O(h_{X,M}), & \left| \sqrt{\det(g_{\gamma_{x_i}})} - \sqrt{\det(g_{\alpha_{x_i}})} \right| &= O(h_{X,M}). \end{aligned}$$

Combining these estimates, simple algebraic manipulations show that

$$\left| \left\langle (\nabla W)_{\gamma_{x_i}}, (\nabla W)_{\gamma_{x_i}} \right\rangle_{g_{\gamma_{x_i}}} \sqrt{\det(g_{\gamma_{x_i}})} - \left\langle (\nabla \widehat{W})_{\alpha_{x_i}}, (\nabla \widehat{W})_{\alpha_{x_i}} \right\rangle_{g_{\alpha_{x_i}}} \sqrt{\det(g_{\alpha_{x_i}})} \right| = O(h_{X,M}),$$

and therefore that

$$\left| \int_{T_{i,r}} \left[\left\langle (\nabla W)_{\gamma_{x_i}}, (\nabla W)_{\gamma_{x_i}} \right\rangle_{g_{\gamma_{x_i}}} \sqrt{\det(g_{\gamma_{x_i}})} - \left\langle (\nabla \widehat{W})_{\alpha_{x_i}}, (\nabla \widehat{W})_{\alpha_{x_i}} \right\rangle_{g_{\alpha_{x_i}}} \sqrt{\det(g_{\alpha_{x_i}})} \right] dv_1 dv_2 \right| = O(\text{Vol}(T_{i,r}) h_{X,M}).$$

This completes the proof. \square

Proof of Corollary 4.1. Let \mathbf{D}^{-1} be the diagonal matrix with entries $(\mathbf{D}^{-1})_{di+1, di+1}, \dots, (\mathbf{D}^{-1})_{di+d, di+d} = \frac{1}{\text{Vol}(R(i))}$. Denote by \mathbf{W} the vector of length dN with entries given by

$$\begin{pmatrix} (\mathbf{W})_{2i+1} \\ (\mathbf{W})_{2i+2} \end{pmatrix} = (\mathbf{t}_1^{(i)})^\top W(x_i) \mathbf{t}_1^{(i)} + (\mathbf{t}_2^{(i)})^\top W(x_i) \mathbf{t}_2^{(i)}$$

From Lemmas 4.1, we have, by construction, that

$$\left| \int_M \langle \nabla W, \nabla W \rangle_g d\text{Vol} - \langle \mathbf{D}^{-1} \mathbf{S} \mathbf{W}, \mathbf{W} \rangle \right| = O(N^{-1/2}) + O(h_{X,M})$$

$$\left| \int_M \langle W, W \rangle_g d\text{Vol} - \langle \mathbf{D}^{-1} \mathbf{M} \mathbf{W}, \mathbf{W} \rangle \right| = O(N^{-1/2}) + O(h_{X,M})$$

with probability higher than $1 - \frac{4}{N}$. Combining the above, we see that

$$\left| \frac{\int_M \langle \nabla W, \nabla W \rangle_g d\text{Vol}}{\int_M \langle W, W \rangle_g d\text{Vol}} - \frac{\langle \mathbf{D}^{-1} \mathbf{S} \mathbf{W}, \mathbf{W} \rangle}{\langle \mathbf{D}^{-1} \mathbf{M} \mathbf{W}, \mathbf{W} \rangle} \right| = O(N^{-1/2}) + O(h_{X,M}).$$

Let S'_ℓ be a subspace of $\mathfrak{X}(M)$ of dimension ℓ on which the quantity $\max_{W \in S'_\ell} \frac{\langle \mathbf{D}^{-1} \mathbf{S} \mathbf{W}, \mathbf{W} \rangle}{\langle \mathbf{D}^{-1} \mathbf{M} \mathbf{W}, \mathbf{W} \rangle}$ achieves its minimum. We have that

$$\max_{W \in S'_\ell} \frac{\int_M \langle \nabla W, \nabla W \rangle_g d\text{Vol}}{\int_M \langle W, W \rangle_g d\text{Vol}} \leq \max_{W \in S'_\ell} \frac{\langle \mathbf{D}^{-1} \mathbf{S} \mathbf{W}, \mathbf{W} \rangle}{\langle \mathbf{D}^{-1} \mathbf{M} \mathbf{W}, \mathbf{W} \rangle} + O(N^{-1/2}) + O(h_{X,M}).$$

Since S'_ℓ is the subspace on which $\max_{W \in S'_\ell} \frac{\langle \mathbf{D}^{-1} \mathbf{S} \mathbf{W}, \mathbf{W} \rangle}{\langle \mathbf{D}^{-1} \mathbf{M} \mathbf{W}, \mathbf{W} \rangle}$ achieves its minimum,

$$\max_{W \in S'_\ell} \frac{\int_M \langle \nabla W, \nabla W \rangle_g d\text{Vol}}{\int_M \langle W, W \rangle_g d\text{Vol}} \leq \min_{S_\ell \in \mathcal{G}_\ell} \max_{W \in S_\ell} \frac{\langle \mathbf{D}^{-1} \mathbf{S} \mathbf{W}, \mathbf{W} \rangle}{\langle \mathbf{D}^{-1} \mathbf{M} \mathbf{W}, \mathbf{W} \rangle} + O(N^{-1/2}) + O(h_{X,M}).$$

Since

$$\lambda_\ell^N = \min_{S_\ell \in \mathcal{G}_\ell} \max_{W \in S_\ell} \frac{\langle \mathbf{A} \mathbf{W}, \mathbf{W} \rangle}{\langle \mathbf{B} \mathbf{W}, \mathbf{W} \rangle} = \min_{S_\ell \in \mathcal{G}_\ell} \max_{W \in S_\ell} \frac{\langle \mathbf{S} \mathbf{W}, \mathbf{W} \rangle}{\langle \mathbf{M} \mathbf{W}, \mathbf{W} \rangle} = \min_{S_\ell \in \mathcal{G}_\ell} \max_{W \in S_\ell} \frac{\langle \mathbf{D}^{-1} \mathbf{S} \mathbf{W}, \mathbf{W} \rangle}{\langle \mathbf{D}^{-1} \mathbf{M} \mathbf{W}, \mathbf{W} \rangle},$$

it follows that

$$\max_{W \in S'_\ell} \frac{\int_M \langle \nabla W, \nabla W \rangle_g d\text{Vol}}{\int_M \langle W, W \rangle_g d\text{Vol}} \leq \lambda_\ell^N + O(N^{-1/2}) + O(h_{X,M}).$$

Minimizing the left-hand-side over all ℓ -dimensional subspaces of $\mathfrak{X}(M)$ yields

$$\lambda_\ell \leq \lambda_\ell^N + O(N^{-1/2}) + O(h_{X,M}).$$

The argument for the other direction $\lambda_\ell^N \leq \lambda_\ell + O(h_{X,M})$ is identical, and hence

$$|\lambda_\ell - \lambda_\ell^N| = O(N^{-1/2}) + O(h_{X,M}),$$

which was to be demonstrated. \square

References

- [1] Mikhail Belkin and Partha Niyogi. Laplacian eigenmaps for dimensionality reduction and data representation. *Neural computation*, 15(6):1373–1396, 2003.
- [2] Mikhail Belkin and Partha Niyogi. Convergence of laplacian eigenmaps. *Advances in Neural Information Processing Systems*, 19:129, 2007.
- [3] Tyrus Berry and Dimitrios Giannakis. Spectral exterior calculus. *Communications on Pure and Applied Mathematics*, 73(4):689–770, 2020.
- [4] Tyrus Berry and John Harlim. Variable bandwidth diffusion kernels. *Applied and Computational Harmonic Analysis*, 40(1):68–96, 2016.
- [5] Marcelo Bertalmio, Andrea L Bertozzi, and Guillermo Sapiro. Navier-stokes, fluid dynamics, and image and video inpainting. In *Proceedings of the 2001 IEEE Computer Society Conference on Computer Vision and Pattern Recognition. CVPR 2001*, volume 1, pages I–I. IEEE, 2001.
- [6] Marcelo Bertalmio, Li-Tien Cheng, Stanley Osher, and Guillermo Sapiro. Variational problems and partial differential equations on implicit surfaces. *J. Comput. Phys.*, 174(2):759–780, 2001.

- [7] Susanne C Brenner. *The mathematical theory of finite element methods*. Springer, 2008.
- [8] J. Calder and N. García Trillos. Improved spectral convergence rates for graph laplacians on ϵ -graphs and k -nn graphs. *arXiv preprint*, 2019.
- [9] Emmanuel J Candès, Xiaodong Li, Yi Ma, and John Wright. Robust principal component analysis? *Journal of the ACM (JACM)*, 58(3):1–37, 2011.
- [10] Ronald R Coifman and Stéphane Lafon. Diffusion maps. *Appl. Comput. Harmon. Anal.*, 21(1):5–30, 2006.
- [11] James W Demmel. *Applied numerical linear algebra*. SIAM, 1997.
- [12] J Dogel, R Tsekov, and W Freyland. Two-dimensional connective nanostructures of electrodeposited Zn on Au (111) induced by spinodal decomposition. *J. Chem. Phys.*, 122(9):094703, 2005.
- [13] David L Donoho and Carrie Grimes. Hessian eigenmaps: Locally linear embedding techniques for high-dimensional data. *Proceedings of the National Academy of Sciences*, 100(10):5591–5596, 2003.
- [14] Richard J Duffin. Distributed and lumped networks. *Journal of Mathematics and Mechanics*, pages 793–826, 1959.
- [15] Charles M Elliott and Björn Stinner. Modeling and computation of two phase geometric biomembranes using surface finite elements. *J. Comput. Phys.*, 229(18):6585–6612, 2010.
- [16] John Harlim, Shixiao Willing Jiang, and John Wilson Peoples. Radial basis approximation of tensor fields on manifolds: from operator estimation to manifold learning. *Journal of Machine Learning Research*, 24(345):1–85, 2023.
- [17] Shixiao Willing Jiang, Rongji Li, Qile Yan, and John Harlim. Generalized finite difference method on unknown manifolds. *Journal of Computational Physics*, 502:112812, 2024.
- [18] Rongjie Lai, Jiang Liang, and Hongkai Zhao. A local mesh method for solving pdes on point clouds. *Inverse Problems & Imaging*, 7(3), 2013.
- [19] Peter D Lax. *Linear algebra and its applications*, volume 78. John Wiley & Sons, 2007.
- [20] Jian Liang, Rongjie Lai, Tsz Wai Wong, and Hongkai Zhao. Geometric understanding of point clouds using laplace-beltrami operator. In *2012 IEEE conference on computer vision and pattern recognition*, pages 214–221. IEEE, 2012.
- [21] Jian Liang and Hongkai Zhao. Solving partial differential equations on point clouds. *SIAM Journal on Scientific Computing*, 35(3):A1461–A1486, 2013.
- [22] Colin B Macdonald and Steven J Ruuth. The implicit closest point method for the numerical solution of partial differential equations on surfaces. *SIAM J. Sci. Comput.*, 31(6):4330–4350, 2010.
- [23] Facundo Mémoli, Guillermo Sapiro, and Paul Thompson. Implicit brain imaging. *NeuroImage*, 23:S179–S188, 2004.
- [24] Davoud Mirzaei, Robert Schaback, and Mehdi Dehghan. On generalized moving least squares and diffuse derivatives. *IMA Journal of Numerical Analysis*, 32(3):983–1000, 2012.
- [25] Ingo Nitschke, Sebastian Reuther, and Axel Voigt. Liquid crystals on deformable surfaces. *Proc. Roy. Soc. Edinburgh Sect. A*, 476(2241):20200313, 2020.
- [26] Matthias Rauter and Željko Tuković. A finite area scheme for shallow granular flows on three-dimensional surfaces. *Comput. & Fluids*, 166:184–199, 2018.
- [27] Zuoqiang Shi, Stanley Osher, and Wei Zhu. Weighted nonlocal Laplacian on interpolation from sparse data. *J. Sci. Comput.*, 73(2):1164–1177, 2017.
- [28] A. Singer. From graph to manifold laplacian: the convergence rate. *Applied and Computational Harmonic Analysis*, 21(1):128–134, 2006.
- [29] Amit Singer and H-T Wu. Vector diffusion maps and the connection laplacian. *Communications on pure and applied mathematics*, 65(8):1067–1144, 2012.
- [30] Amit Singer and Hau-Tieng Wu. Spectral convergence of the connection Laplacian from random samples. *Information and Inference: A Journal of the IMA*, 6(1):58–123, 2017.
- [31] Li Tian, Colin B Macdonald, and Steven J Ruuth. Segmentation on surfaces with the closest point method. In *2009 16th IEEE International Conference on Image Processing (ICIP)*, pages 3009–3012. IEEE, 2009.
- [32] Hemant Tyagi, Elif Vural, and Pascal Frossard. Tangent space estimation for smooth embeddings of riemannian manifolds. *Information and Inference: A Journal of the IMA*, 2(1):69–114, 2013.

- [33] Yubin Zhan and Jianping Yin. Robust local tangent space alignment via iterative weighted pca. *Neurocomputing*, 74(11):1985–1993, 2011.
- [34] Zhenyue Zhang and Hongyuan Zha. Principal manifolds and nonlinear dimensionality reduction via tangent space alignment. *SIAM journal on scientific computing*, 26(1):313–338, 2004.
- [35] Hong-Kai Zhao, Stanley Osher, and Ronald Fedkiw. Fast surface reconstruction using the level set method. In *Proceedings IEEE Workshop on Variational and Level Set Methods in Computer Vision*, pages 194–201. IEEE, 2001.